This is to certify that the
thesis entitled

EFFECTS OF CHRONIC CARBON BLACK PARTICLE
INHALATION ON THE NASAL AIRWAYS OF LABORATORY
RODENTS: A SPECIES COMPARISON

presented by

PRIYA SANTHANAM

has been accepted towards fulfillment
of the requirements for the

MS degree in Pathology

Major Professor's Signature

6/30/04

Date

MSU is an Affirmative Action/Equal Opportunity Institution

EFFECTS OF CHRONIC CARBON BLACK PARTICLE INHALATION ON THE NASAL AIRWAYS OF LABORATORY RODENTS: A SPECIES COMPARISON

By

Priya Santhanam

A THESIS

Submitted to
Michigan State University
in partial fulfillment of the requirements
for the degree of

MASTER OF SCIENCE

Department of Pathobiology and Diagnostic Investigation

2004

ABSTRACT

EFFECTS OF CHRONIC CARBON BLACK PARTICLE INHALATION ON THE NASAL AIRWAYS OF LABORATORY RODENTS: A SPECIES COMPARISON

By

Priya Santhanam

The effects of chronic exposure to carbon black (Cb) on the nasal airways of laboratory rodents have not been previously investigated. The purpose of the present study was to determine if long-term inhalation of Cb would cause chronic lesions in the nasal airways of rats, mice, and hamsters. Chronic active rhinitis and persistent mucous cell metaplasia (MCM) and hyperplasia (MCH) with increased mucous cells were present in rats exposed to mid and high concentrations of a high surface area Cb (HSCb). In contrast, rats exposed to the high concentration of low surface area Cb (LSCb) had no nasal lesions in any region of nasal epithelium. Mice exposed to mid and high concentrations of HSCb had similar but less severe and transient rhinitis, MCM, and MCH. Interestingly, hamsters exposed to similar concentrations of HSCb did not develop rhinitis or MCM, but rather only mild MCH in one region of nasal epithelium. The results of this study indicate that Cb-induced nasal lesions were dependent on species, particle surface area, dose, and time post-exposure.

To Amma and Appa,

who always supported me.

ACKNOWLEDGEMENTS

In my years at Michigan State University I have relied on the help and support of many, and I owe any and all of my success to those who surrounded me during this time. First of all, I would like to thank my advisor and mentor, Dr. Jack Harkema. When I decided to change my career path, Dr. Harkema was willing to take me under his wing full time and allow me to pursue my research project in a concentrated and in-depth manner. I learned a vast amount about the world of scientific research from the opportunities he gave me, including presenting at poster sessions and attending national meetings. I am a better writer, researcher, and thinker because of his guidance in these past two years.

Next on the list (and if I did not place him here I would never hear the end of it) is Dr. Jim Wagner. Jim helped me in countless ways to adjust to my new environment when I first joined the lab. His invaluable advice on the pressures of graduate school and how to deal with them has taught me lessons I will not soon forget, and plan to carry with me in my further pursuits. Of course Jim was more than just a go-to person for my technical questions; his sense of humor and easy-going style made me feel comfortable enough to make myself at home in his office chair anytime I needed to. I am indebted to him for all his advice and support.

Additionally, I want to especially thank the head technician of the Harkema lab, Ms. Lori Bramble. Lori has been a helping-hand and a friend and confidant

ever since I joined the lab. She was always encouraging when I struggled, and I will forever remember how her kindness aided me in keeping high hopes. I owe a great deal of my success in this project to her. I also would like to thank the rest of the technical staff in the Harkema lab and the MSU histology lab. I would never have managed this project without their help. My gratitude also goes to the "eagles and crows" of my thesis committee, including Drs. Ed Robinson and Sue Ewart, for their constructive analyses of my written work.

Finally, I would like to thank my family for their undying encouragement and support, no matter what I chose to pursue in my time at MSU. I would not have the analytical capacity to pursue these higher educational goals if not for the teachings they have bestowed on me ever since I took my first steps.

To all those mentioned above, I owe the success of this project and my potential.

TABLE OF CONTENTS

LIST OF FIGURES

LIST OF ABBREVIATIONS

AAMs	Arachadonic acid metabolites
AB/PAS	Alcian blue/periodic acid-Schiff
BrdU	Bromodeoxyuridine
Cb	Carbon black particles
CFD	Computational fluid dynamics
COPD	Chronic Obstructive Pulmonary Disease
CV	Cardiovascular
DEP	Diesel exhaust particles
ECH	Epithelial cell hyperplasia
GSD	Geometric standard deviation
H&E	Hematoxylin & Eosin
HSCb	High-surface area carbon black
IM	Intraepithelial mucosubstances
LSCb	Low-surface area carbon black
MCH	Mucous cell hyperplasia
MCM	Mucous cell metaplasia
NALT	Nasal associated lymphoid tissue
NOAEL	No Observable Adverse Effect Level
NPM	Nasopharyngeal meatus
NTE	Nasal transitional epithelium
OE	Olfactory epithelium
OVA	Ovalbumin
PE	Post-exposure
PM	Particulate Matter
PSPs	Poorly soluble particles
RE	Respiratory epithelium
ROS	Reactive oxygen species
RSV	Respiratory syncitial virus
SE	Squamous epithelium
TNF	Tumor necrosis factor
UF	Ultrafine
Vs	Volume density

CHAPTER 1

Introduction

I. Carbon Black

A. Carbon Black Particles

Description

Carbon black is elemental carbon with few or no organic components that is produced by the controlled combustion of gaseous or liquid hydrocarbons. Although there are many types of carbon black, more than 90% of manufactured carbon black is "furnace black," which is produced by the incomplete, controlled combustion of natural gas. Manufactured carbon black is produced by pumping petroleum-based oil into a furnace, which creates a stream of gas and powder that get separated by a series of filters [1]. The carbon powder produced is what is known as carbon black [1].

Manufacturing and Uses

Packaging of carbon black by manufacturers involves binding the carbon powder form to water, drying, and packing the compound in the form of granules. Most types of manufactured carbon black contain 97-99% elemental carbon, but sometimes the powder can contain attached chemical groups such as hydrogen, oxygen, nitrogen, and sulfur. These groups create variations in the surface chemistry of the particles. Bound oxygen is of particular importance, since it serves as a functional group that binds hazardous compounds like carcinogenic polycyclic aromatic hydrocarbons.

Carbon black is primarily used as a reinforcing agent in the industrial manufacturing of rubber and automotive products such as tires, gaskets, and hoses. Smaller amounts of carbon black are also found as pigments for paints, plastics, and inks.

In addition, carbon black, also called elemental carbon, is found in the environment as the inorganic core component of diesel engine exhaust particles that are found in particulate air pollution [2-4]. Elemental carbon has been reported to comprise 45-85% of diesel exhaust particulate matter, depending on the type of engine [5].

Particle Characterization

Carbon black particles are characterized by the size and surface area of the primary particle, as well as by their degree of agglomeration in air. While the primary particle diameter is in the nanometer range, the nature of these slightly charged particles is to fuse together during generation or aerosolization to produce small clusters of particles called aggregates that are up to one to two microns in size. It is hypothesized that the clusters remain intact during inhalation as long as the particles are airborne and even remain in aggregates if inhaled and deposited in the respiratory tract [6]. Controlled combustion during manufacturing results in variation of parameters, such as size and surface area, of the different types of carbon black. Manufactured carbon black varies in size from 10-400 nm primary particle diameter, and has an average aggregate diameter of 100-800 nm [7].

B. Human Exposure

Occupational Exposure

Exposure Concentrations and Regulations

Human exposure to airborne carbon black particle concentrations is primarily occupational. The German inhalable standard for workplace concentrations is 4.0 mg/m^3 (German MAK), while the US inhalable occupational standard is 3.5 mg/m^3 (Occupational Safety and Health Administration; OSHA). Carbon black-induced adverse health effects in the workplace appear to be limited to non-neoplastic effects, as there is "inadequate evidence for the carcinogenicity in humans of carbon black" [7]. A survey of total and respirable carbon black dust concentration was conducted from 1993-1995 in all major US carbon black production plants [8]. In this study it was determined that the average total carbon black concentration was approximately 0.6 mg/m^3, while the respirable concentration was approximately 0.2 mg/m^3.

Human Exposure Studies

There have been a few cohort studies designed to determine the adverse health effects in workers chronically exposed to carbon black. One survey of industrial workers in the United Kingdom occupationally exposed to carbon black found a statistically significant number of deaths of these workers was due to malignant neoplasms and respiratory cancer as compared to general population controls [9]. A Canadian community study indicated a correlation between lung cancer and chronic carbon black exposure for painters and rubber industry workers [10].

The investigators of these two studies admit, however, that lack of case-control in the studies renders their findings as insufficient evidence for excess risk to lung cancer by carbon black exposure [9, 10]. The discrepancy among carcinogenicity studies may be due to the changes instituted in the past 50 years in production and control processes in carbon black manufacturing plants, resulting in substantial declines in occupational exposure [8]. Therefore these modifications in industry may have eliminated the risk of carbon black as a human lung carcinogen, and the compound is not classified as a human carcinogen today [7]. Two more recent studies from 2001 conducted in the US and UK found adverse physiologic effects in chronically exposed carbon black workers [11]. Both studies reported a significant decrease in forced expiratory volume in one second in chronically exposed carbon black plant workers. Additionally, the US survey showed a correlation between carbon black exposure and chronic bronchitis [11]. However, neither recent study found any other adverse effect, such as carcinogenic potential, in the chronically exposed workers.

Environmental Exposure

While there are no national ambient air quality standards for carbon black, it does exist in the environment as the core inorganic component of diesel engine exhaust and in other airborne particles arising from the tires of motor vehicles.

Ambient Concentrations

Several studies have been conducted to examine the concentration of various components of ambient particulate matter, including elemental carbon concentrations. An air quality study in Fresno, CA measured elemental carbon in mass concentrations up to 7% of the total ambient particulate matter [12]. Daily mean ambient concentrations of inorganic carbon have been reported to be 1.5 $\mu g/m^3$ in low-traffic environments and up to 10 $\mu g/m^3$ in high-traffic zones [2]. One study of elemental carbon concentrations along a truck route in New York City reported daily mean control concentrations at 2.6 $\mu g/m^3$ and high-traffic region concentrations at 7.3 $\mu g/m^3$ [3]. Additionally, a study of trucking industry worker exposure to diesel exhaust particles determined respirable elemental carbon concentrations within the diesel particles to be significantly lower in normal traffic regions versus high-truck volume areas [4]. Zaebst, et al. reported daily mean control carbon concentrations to be 1.1 $\mu g/m^3$ in residential areas and 2.5 $\mu g/m^3$ along the highway, while mean exposures to truck drivers was 3.8 $\mu g/m^3$ and to dock workers was 13.8 $\mu g/m^3$.

Diesel Combustion Effect

Since estimated concentrations of elemental carbon in ambient air have been reported to vary with traffic density, variations in the amount of diesel exhaust particulate can often account for differences in measured ambient carbon concentrations. While diesel concentrations can obviously vary with degree of diesel combustion in the region, another reason for the difference can be changes in the composition of the diesel exhaust itself. It is known that the makeup of diesel exhaust particulate varies depending on the conditions under which it is generated [13]. For example, the US EPA reported that the elemental carbon percentage of diesel exhaust is approximately 75% from a heavy-duty diesel engine, but only 60% from a light-duty diesel engine [5]. Therefore, the type of diesel engine may account for differences in elemental carbon concentrations among high-exposure regions.

C. Animal Studies

Pulmonary Toxicity

Laboratory Rodents: Rats

Several in vivo and in vitro studies suggest that the pulmonary airways of laboratory rodents are susceptible to carbon black toxicity. Chronic exposure studies using particle concentrations varying from 4-105 mg/m^3 have demonstrated increased lung weights, type II cell hyperplasia, neutrophilic influx, squamous metaplasia, bronchial epithelial cell hyperplasia, and lipoproteinosis in the lungs of exposed rats. Furthermore, chronic exposure of rats to carbon black at extremely high concentrations induces pulmonary tumors [14-16].

1. Neoplastic Lesions

Mauderly, et al. have reported a significant incidence of lung neoplasms in male and female F344 rats with inhalation exposure to 6.5 mg/m^3 carbon black for 16 hours/day, 5 days/wk for up to 24 months [16]. Furthermore, the prevalence of neoplasms increased with the duration of exposure, appearing in 20% of rats at 650 days after the start of exposure and increasing to 70% of rats by 770 days into the exposure. Nikula, et al. designed an exposure regimen of similar dosage and duration as Mauderly, et al. for rats, and found a significant prevalence of lung adenocarcinomas in female rats exposed chronically to carbon black [15]. Additionally, Heinrich, et al. reported that similarly exposed female Wistar rats develop benign pulmonary squamous tumor cysts, keratin cysts, and adenomas, as well as malignant adenocarcinomas and squamous cell carcinomas [17].

Laboratory rodents also develop tumorigenic lung lesions induced by intratracheal instillation of carbon black. In a study by Rittinghausen, et al., female Wistar rats had an increased incidence of benign and malignant tumors upon intratracheal administration of extracted carbon black particles [18]. Specifically, 19% of rats exposed to extracted carbon black particles developed cystic keratinizing squamous cell carcinomas, while 16% of rats exposed to nonextracted carbon black developed cystic keratinizing epitheliomas.

2. Non-Neoplastic Lesions

Carbon black particles have also been shown to induce a number of nonneoplastic lesions in the pulmonary airways of laboratory animals. Several authors have reported pulmonary injury in rats after exposure to 6.5-7.5 mg/m^3 carbon black for 16-18 hours/day, 5 days/week, for 24 months [14-16]. Chronic alveolitis, alveolar septal fibrosis, and type II cell hyperplasia were commonly found in the pulmonary parenchyma. Driscoll, et al. reported genotoxicity of alveolar epithelial cells and pulmonary inflammation as indicated by increased cytokine and growth factor expression in rats exposed to carbon black [14]. The carbon black-induced inflammatory response was hypothesized to activate alveolar macrophages leading to overproduction of reactive oxygen species, resulting in further lung injury [19].

Mauderly, et al. has described the stages of progression of lung lesions associated with chronic carbon black inhalation in rats [16]. Within 3 months of exposure, rats exposed to 6.5 mg/m^3 carbon black had an increase in the number of particle-containing alveolar macrophages, aggregated in the centriacinar region. Alveolar epithelial hyperplasia and alveolitis, as indicated by inflammatory cell influxes, were also present in these rats after 3 months of exposure. Interstitial fibrosis developed after 6-12 months of exposure, followed by bronchiolar-alveolar and squamous metaplasia, and finally leading to the appearance of tumors around 18-24 months of exposure. In all of the preceding studies, increases in the number, size, and severity of histopathological lesions induced by carbon black correlated with increases in concentration of particles administered to the rats [14-16].

A recent study conducted by Oberdorster, et al. involved the exposure of rats to 0, 1, 7, or 50 mg/m^3 carbon black for 6 hours/day, 5 days/week, for 13 weeks [20]. Immediately at the end of exposure as well as 11 months post-exposure, the investigators found increased lung lavage neutrophil counts and the formation of a known mutagenic lesion [8-oxo-7,8-dihydro-2'-deoxyguanosine (8-oxo-dG)] in the lung DNA of rats exposed to 50 mg/m^{3}carbon black.

Histopathologic lesions included severe and persistent alveolitis and alveolar epithelial proliferation, characterized by type II cell hyperplasia, in rats exposed to the high carbon black exposure concentration [21].

Common to most carbon black-exposed rats in the previously mentioned chronic studies were impaired normal particle clearance and particle accumulation that was progressive with time [15, 16]. At high concentrations, inhaled carbon black particles are known to overload the defense capability of the lung by impairing the ability of alveolar macrophages to perform essential cytoskeletal functions such as phagocytosis [22-24]. Many investigators have reported a correlation between increased carbon black exposure concentration and impaired lung clearance, resulting in higher lung burden in rats exposed to carbon black concentrations ranging from 7-50 mg/m^3 [14, 15]. Since carbon black-induced neoplastic lung lesions are observed only in the presence of particle overload conditions, it is thought that impaired clearance contributes to the induction of progressive inflammatory and tumorigenic pathways in chronically exposed animals [25].

Short-term carbon black exposure can also induce lung injury in rats. Gilmour, et al. found inflammatory indicators in the lungs of rats exposed by inhalation to ultrafine carbon black particles for 7 hours and sacrificed immediately after exposure [26]. Specifically, the authors showed an increase in total lung lavage leukocytes and neutrophils, as well as increased proinflammatory cytokine levels in lavage cells of the rats. In another acute study, intratracheal instillation of 35 mg/kg carbon black particles in rats attenuated the activity of antioxidant enzymes (e.g., CYP2B1, GST, catalase), which are associated with detoxification in the lung [27]. Yet another study reported lung inflammation and oxidative stress caused by a low dosage (125 µg) of carbon black administered by intratracheal instillation [28].

Laboratory Rodents: Mice

One study using an in vitro murine alveolar epithelial cell line reported an increase in the expression of protooncogenes and cell proliferation after carbon black particle administration [29]. Several of the previously mentioned in vivo rodent studies also examined lung injury in mice chronically exposed by inhalation to carbon black particles. However, no study indicated more than minimal lung response in mice. No neoplastic or tumorigenic lesions were found in mice exposed to concentrations of carbon black similar to those that induced tumors in rats, even though the mice developed overload conditions similar to those in the rats [15, 16]. Only the recent study by Oberdorster, et al. found an increase in lung lavage neutrophils immediately post-exposure in $B_6C_3F_1$ mice exposed to 50 mg/m^3 carbon black [30]. While the increase in neutrophils was significant in these mice as compared to air-exposed control animals, the neutrophil response in similarly exposed F344 rats was markedly greater and more prolonged than that in the exposed mice.

Non-Human Primates

Only one study to date has examined the effects of carbon black inhalation on the pulmonary airways of non-human primates. Nau, et al. exposed monkeys by inhalation to a moderate concentration of particles continuously for three years [31]. The animals appeared to have emphysema-like lesions at the end of exposure, limited to the centriacinar region of the lungs. Inflammation and tumor formation were not primary conclusions from this single study, however. It has been suggested that one reason for the differences in lung response to inhaled insoluble particles, such as carbon black, between rodents and monkeys is a difference in standard load volume of particles per pulmonary macrophage. Lab rodent macrophages are about half the volume of monkey macrophages, allowing for much greater susceptibility of rodents to volumetric loading by particles and subsequent overload conditions [32].

Humans

There have not been many studies examining the toxicity of carbon black to the pulmonary airways of humans. Aside from the epidemiological studies previously mentioned examining the chronic effects of occupational exposure, the rest of the studies of carbon black have been in vitro studies using human cell lines or extracts. One study reported the effects of carbon black particles on stimulation of peripheral neutrophils from chronic obstructive pulmonary disease (COPD) patients versus those from healthy individuals [33]. Van Beurden, et al. demonstrated that ultrafine carbon black particles stimulated the release of oxidants in vitro, specifically of superoxide anions, from neutrophils collected from COPD patients but not by neutrophils from healthy people, critically linking neutrophil activation to particle exposure. In another study, inhibition of tissue repair was evidenced upon exposure to carbon black particles by inhibited contraction of an artificial 3-D collagen gel model containing fibroblast cells [34]. Finally, a third study utilized two human cell lines, alveolar epithelial and monocytic, to determine the effects of carbon black particles on human lung tissue [35]. In both cell lines, but more so in the monocyte line, genotoxicity was indicated by DNA damage due to carbon black exposure. According to the authors, the contribution of carbon black particles to DNA damage in human pulmonary cell lines may implicate them in the first stages of tumor formation [35].

Cb Enhancement of Pulmonary Pathology

Allergic Airway Sensitization

Carbon black is known to enhance the adverse effects of other pulmonary irritants. One of the most well-documented effects is the role of carbon black particles in the enhancement of allergic airway sensitization. Al-Humadi et al. has reported an enhanced allergic response, characterized by increases in cytokine expression and serum IgE levels, in mice dually administered carbon black and ovalbumin (OVA), an airway allergen [36]. Another study involved administration of OVA and carbon black particles intranasally to mice, and reported an elevation in OVA-specific IgE levels in serum versus mice given only OVA [37]. Van

Zijuerden, et al. reported on the differences in enhancement of allergic sensitization depending on when the carbon black was administered [38]. They demonstrated an enhanced allergic response in mice when carbon black was given just before OVA sensitization, but not when given just before OVA challenge. However, the optimal allergic response model was seen when carbon black and OVA were coadministered at all dosages during the sensitization phase. The results of these experiments suggest that there are time-dependent processes involved in the immune-stimulating activity of particles [38]. The authors further determined that carbon black and OVA together induced a mix of Th1 and Th2 immune responses in the lungs of the allergic mice [39]. Other studies have reported that the organic and inorganic (elemental carbon) components of diesel exhaust, when coadministered, may further enhance respiratory OVA allergic sensitization [19, 36, 40].

Viral Infection

Intratracheal administration of carbon black 3 days after respiratory syncitial virus (RSV) infection led to the development of an enhanced viral infection in mice as compared to mice exposed to just RSV [41]. This demonstrates a synergistic effect of carbon black on RSV infection, and suggests a potential mechanism for increased respiratory tract infections after exposure to ambient particulate matter [41]. Carbon black has also been shown to induce an immune response in mice, characterized by increased Th2 proinflammatory cytokine levels, when administered intratracheally just before RSV [40]. This Th2-response was observed in place of the microbial defense mechanisms which were observed with RSV administration alone.

Ozone

Pulmonary toxicity of ozone may be enhanced by carbon black particles. Jakab, et al. coexposed mice to 10 mg/m^3 carbon black and 1.5 ppm ozone, or to just carbon black or ozone, for 4 hours [42]. At 24 hours post-exposure mice exposed to ozone had increased inflammatory responses and decreased alveolar macrophage phagocytosis. Mice coexposed to carbon black and ozone had the same pulmonary responses as those exposed only to ozone but the effects were significantly enhanced. Kleinman, et al. also showed more severe losses in lung collagen and repair-related cell proliferation in rats coexposed to carbon black and ozone than rats exposed only to ozone [43].

Extrapulmonary Translocation

Translocation of inhaled particles and other compounds to organs outside of the respiratory tract often occurs post-exposure. Examples of this include beryllium oxide particles, ultrafine iridium particles, and plutonium oxides, all of which are found in the liver of rats after acute inhalation exposure and deposition in the lung [44-46]. The iridium particles have also been shown to translocate to the heart and brain in acutely exposed rats [46]. Additionally, inhaled metal dusts and aerosols, for example manganese, nickel, and zinc, are known to translocate from the nasal mucosa to the olfactory bulb of the brain in rats [47]. Similarly, by way of extrapulmonary translocation, inhaled carbon black particles may accumulate in other organs besides the lungs of laboratory rodents.

Liver

One organ that may be affected by systemic translocation of carbon black is the liver. Oberdorster et al. demonstrated effective translocation of carbon black particles to the liver from the pulmonary airways of exposed rats [48]. Carbon black particle burden in the liver was measured by performing mass spectroscopy on homogenized tissue after rats were inhalation exposed to radiolabeled carbon particles. Significant liver burden of carbon particles was observed in rats within one day after a 6 hr whole-body inhalation exposure. Furthermore, by 18 hours post-exposure, all exposed rats exhibited a 5-fold increase in liver burden of particles versus the lungs. Another study by Khandoga, et al. demonstrated procoagulation factor release in the liver of mice exposed by inhalation to carbon black, but no inflammatory reaction or tissue damage [49]. The toxic effects of translocated particles as related to hepatic function have not been examined in detail.

Brain

In another study, Oberdorster, et al. reported that ultrafine carbon particles may be translocated to the central nervous system (CNS), specifically the olfactory bulb [50]. In this study, rats were exposed by inhalation to radiolabeled carbon particles, and ^{13}C concentration was examined by mass spectroscopy in homogenized olfactory bulbs from exposed animals. Carbon concentrations were found to be significantly increased in ^{13}C exposed animals vs. control animals. However, the potential toxic effects on the CNS of this movement of carbon black particles via the olfactory nerve are yet to be determined.

Heart

Ambient particulate matter has been implicated in alterations that can lead to heart disease in humans, including changes in heart rate, blood coagulation, and endothelin levels [51-54]. Elemental carbon, as a component of inhaled particulate matter, has been implicated in the increased incidence of cardiovascular (CV) disease in ambiently exposed individuals. Sorensen, et al. found a positive correlation between carbon black exposure and plasma protein oxidation in human blood [55]. Plasma protein oxidation products are an indicator of protein damage, and are potentially related to the induction of CV diseases. Metzger, et al. and Mar, et al. reported correlations between elemental carbon exposure (as a component of particulate matter in polluted US cities) and CV disease hospital visits and CV mortality, respectively [56, 57].

D. Summary

Inert carbon particles, also known as carbon black, are a known respiratory tract irritant. Carbon black exposure can occur occupationally in the manufacturing of rubber and automotive products, as well as environmentally as the inhaled inorganic core component of diesel engine exhaust. The ultrafine size (diameter

< 0.1 μm) of carbon black allows it to deposit in the deep regions of the lung of exposed animals and humans, and many studies have determined it to be a potent pulmonary toxicant. Rats chronically exposed to carbon black particles at very high concentrations are known to undergo particle overload conditions and subsequently develop severe inflammatory and epithelial lesions and pulmonary tumors. However, examination of a distinct correlation between long-term occupational carbon black exposure and the development of lung cancer has been inconclusive to date in the few human cohort studies that have been conducted. Therefore, carbon black is characterized as a known pulmonary carcinogen in lab animals, and a possible human carcinogen [7].

II. Pulmonary Toxicity of Particles

Aside from carbon black, many other particles of various sizes and compositions may cause injury to pulmonary tissues. Environmental exposure to particulate matter, a component of air pollution, and occupational exposure to hazardous ultrafine particles, such as diesel particles and titanium dioxide, are examples of conditions known to induce lung injury in animals and humans.

A. Particulate Matter

One of the most prominent environmental air pollutants is particulate matter. Particulate matter (PM) is the general term used for a mixture of solid particles and liquid droplets found in the air [58]. There are three types of particles in PM: coarse (PM-10; greater than 2.5 μm primary particle diameter), fine (PM-2.5; 1.0 to 2.5 μm), and ultrafine (PM-1.0; less than 1.0 μm) [58]. All three sizes of particles are reported to cause pulmonary inflammation [59, 60].

Airborne particulate matter is known to induce toxic effects on the lungs of lab rodents. Tao, et al. demonstrated that PM can induce alveolar macrophages, epithelial cells, and neutrophils to produce reactive oxygen species (ROS) in vitro, as well as increased cytokines, chemokines, and neutrophil influxes in vivo [61]. Donaldson, et al. reviewed many other studies exhibiting a link between ambient PM and oxidative stress in the lung [62]. According to the authors, oxidative stress created by ROS may be a prominent mechanism of PM-inducing lung inflammation (70, 71).

Coarse

Coarse particles, generally generated from sources such as vehicles traveling on unpaved roads and the breakdown of industrial materials, have been reported to induce proinflammatory reactions in rat lungs in the form of increased cytokine levels in vivo and in vitro [63, 64]. In addition to inflammation in pulmonary cells, Donaldson, et al. reported ROS and free radical formation and DNA damage in vitro [65]. An epidemiology study of PM-10 also reported that human exposure to coarse particles causes chronic cough, bronchitis, chest illness, and increased mortality [66].

Fine

Fine PM, which originates from fuel combustion, power generation, and industrial plants, can cause pulmonary toxicity as well. PM-2.5 has been shown to induce inflammatory responses similar to those seen with exposure to PM-10 in rats, but the more common response is cytotoxicity [67]. Choi, et al. demonstrated apoptosis by means of oxidative stress (increased oxidative enzyme mRNA levels) in rat lung epithelial cells exposed to fine PM in vitro [68].

Ultrafine

Ultrafine PM is thought to deposit in the deepest regions of the lung in animals and humans. A study by Calderon, et al. examined the pulmonary airways of dogs in Mexico City using light and electron microscopy [69]. Interstitial, intravascular, and bronchial wall macrophages all contained ultrafine PM in the dogs. Additionally, the canine lungs had bronchiolar epithelial hyperplasia, peribronchiolar fibrosis, inflammatory cell influxes, and alveolar macrophage proliferation. Another study of ultrafine PM toxicity examined the lungs of children living near and away from main traffic roads in the United Kingdom [70]. Significantly greater numbers of alveolar macrophages, many of them containing ultrafine PM, were found in children living near main traffic roads as compared to children living away from heavy traffic. Additionally, a study conducted on human bronchiolar epithelial cells in vitro demonstrated that ultrafine PM causes increased cytokine production and lipid peroxidation [71].

B. Ultrafine Particle Toxicity

Efficiency of diffusional deposition of coarse, fine, and ultrafine particles varies in the respiratory tract by region. Known patterns of regional particle deposition in the human respiratory tract indicate that ultrafine particles (diameter < 0.1µm) such as carbon black deposit foremost in the pulmonary and nasal airways (Figure 1). In correlation with this information, previous studies have shown ultrafine particles to be the particle type primarily associated with pulmonary toxicity [72]. In fact, many ultrafine poorly soluble particles (PSPs), such as carbon black, diesel exhaust particles, and pigment grade titanium dioxide, are known to cause lung tumors in rats when chronically inhaled at high particle concentrations [73].

Figure 1: Regional Particle Deposition in Human Respiratory Tract; International Commission on Radiological Protection model of aerosol regional deposition with indicated aerodynamic diameter (ICRP, Human Respiratory Tract Model for Radiological Protection, Bd. ICRP Publication 66, Annals of the ICRP, 24,1-3, Elsevier Science, Oxford, 1994)

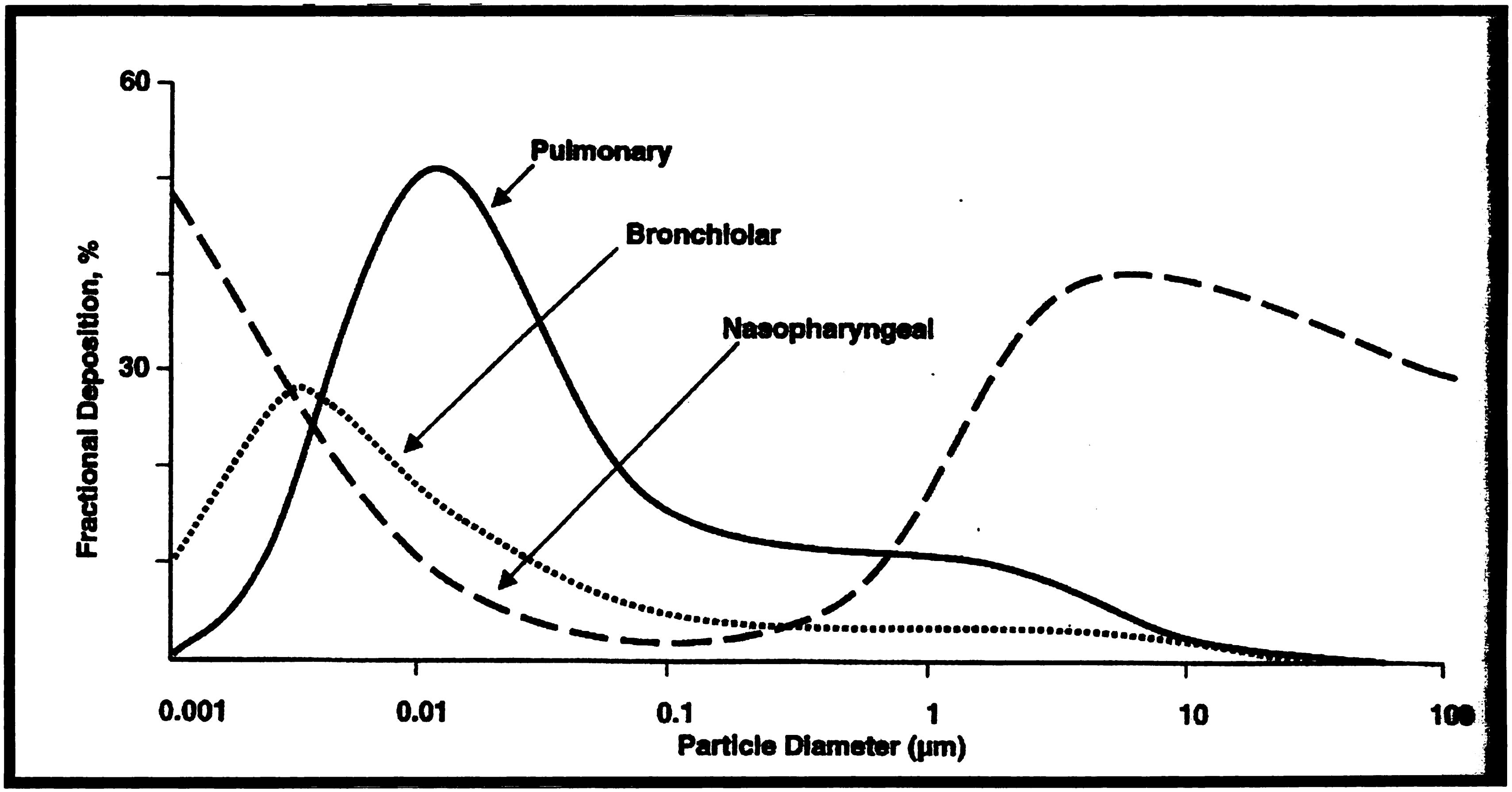

Diesel Exhaust Particles

Diesel exhaust particles (DEP), commonly found environmentally and occupationally, are the particulate byproduct of diesel engine combustion. They have been reported to cause cytoskeletal dysfunctions in canine alveolar macrophages in vitro [24]. Additionally, DEP is known to inhibit cell-mediated immunity, suppress the production of inflammatory cytokines by macrophages, and induce oxidant lung injury via the production of reactive oxygen species in vitro [19]. Rats exposed to high doses of DEP develop similar chronic non-neoplastic pulmonary lesions (e.g., fibrosis, alveolitis, bronchoalveolar epithelial hyperplasia and metaplasia) as those seen in the lungs of rats exposed to high doses of carbon black. The DEP responses appear to occur in a similar manner to carbon black responses, in that both particle types create significant lung burden and overload conditions in exposed rats [15, 16]. The lung tumors, both benign and malignant, observed in rats chronically exposed to high concentrations of DEP are also of similar type and incidence as those found in rats exposed to carbon black [15].

Titanium Dioxide

Titanium dioxide (TiO_2) is a highly studied PSP with respect to pulmonary toxicity and carcinogenicity. Pigment grade TiO_2 (ultrafine) is found as the white pigment in paints, and significant exposure to the pigment is primarily occupational. A chronic inhalation study by Lee, et al. involved the exposure of rats to 250 mg/m^3 TiO_2 for 2 years [74]. The prevalence of bronchiolar adenomas and cystic keratinizing squamous cell carcinomas was significantly higher in exposed rats than in air-exposed controls. Another study by Bermudez, et al. examined the non-neoplastic effects in rats of exposure to 10, 50, or 250 mg/m^3 TiO_2 for 13 weeks [75]. The authors found severe and persistent lesions in the lungs of rats exposed to 50 and 250 mg/m^3 TiO_2, characterized by marked proliferation of alveolar epithelial cells, increases in macrophage and neutrophil counts, and substantial pulmonary particle overload.

Mechanisms of Toxicity

The mechanisms by which ultrafine particles induce significant lung injury are highly speculated. Oberdorster in a review of PSP pulmonary toxicity has divided adverse effects into 4 stages: inflammation, particle kinetics, morphology, and chronic disease [76]. First, inflammatory and lavage parameters increase in the lungs of exposed animals, then particle retention elevates (decreased clearance), cell proliferation initiates, and finally fibrous and tumorigenic lesions develop. However, how particle parameters such as size and surface area affect the severity and incidence of the pathology is still unknown.

1. Influence of Particle Parameters

Two parameters known to influence the incidence of lung burden and lesions in laboratory rodents are size and surface area/mass ratio of the ultrafine particle. In a study of ultrafine TiO_2 in the rat lung it was found that 250 nm-size particles were much less retained in the lung than 20 nm-size particles [77]. The difference in effects were determined by the observation of inhibited alveolar macrophage-mediated particle clearance in rats exposed to the smaller (20 nm) particles, and a 2-fold greater particle retention time than rats exposed to 250 nm particles. However, when two 20 nm-size TiO_2 particles with different surface areas (SA; 20 and 50 cm^2) but equal mass were examined for particle retention time, the 50 cm^2 SA particles had an 8-fold longer retention time vs the 20 cm^2 SA particles [77].

Studies have also demonstrated that particles smaller in size have greater injurious effects than larger particles in the lungs of rats. Brown, et al. observed a significantly greater neutrophilic influx in the pulmonary airways of rats instilled with 64 nm-size polystyrene particles versus rats instilled with 202 nm or 535 nm-size particles [78]. A direct correlation was also found when the surface areas of the polystyrene particles were plotted vs. neutrophil response, with increasing responses to higher surface area particles [78]. Furthermore, inflammatory responses, indicated by lung lavage neutrophils, were increased in the pulmonary airways of animals exposed to ultrafine TiO_2 particles (20 nm) of higher surface area [78]. These and other studies have shown, therefore, a positive correlation between ultrafine TiO_2 and polystyrene particle surface areas and lung injury [77, 79]. While size also appears to affect the toxicity of ultrafine particles, many believe that surface area/mass ratio is a better dose parameter to correlate with inflammatory and other toxic responses [20, 77-79].

2. Speculated Mechanisms

Mechanisms of ultrafine (UF) particle toxicity in the pulmonary airways of lab rodents have been studied extensively. Ultrafine particles are known to induce oxidative stress in the lungs of exposed animals [61, 80, 81]. It is hypothesized that ultrafine particles in particular are able to generate oxidative injury because of their small size, which allows them considerable tissue penetration and subcellular localization [82].

There are two speculated mechanisms by which these particles are thought to induce oxidative stress in pulmonary cells. The first mechanism is via inflammatory mediators, including inflammatory cytokines and signalling processes. UF particles have been shown to induce the release of tumor necrosis factor (TNF) from pulmonary macrophages that is mediated by calcium signalling [80, 83]. TNF, a proinflammatory cytokine, in turn activates more macrophages in the pulmonary airways of exposed animals to release more chemokines and cytokines, including IL-8 [80]. IL-8 is a neutrophilic chemoattractant, and once neutrophils infiltrate the particle-exposed tissue, they are known to release elastase and/or directly generate reactive oxygen species (ROS) [84]. Elastase is a serine protease that impairs mucociliary clearance and stimulates mucous cell metaplasia and mucin production in pulmonary epithelial cells [84]. ROS may in turn enhance intraepithelial mucous synthesis and secretion, as well as upregulate mucin gene expression (Figure 2; [85]).

Direct generation of ROS by particle interaction with the pulmonary tissue is another possible mechanism of ultrafine particle toxicity [78]. This pathway

Figure 2: Speculation on processes that impact mucus obstruction of the airways; Carbon black particles may act via inflammatory mediators or directly induce ROS formation in pulmonary tissues, leading to increased mucin gene expression and goblet cell hyperplasia (Rose, et al, *Am. J. Respir. Cell Mol. Biol.* 25,5: 533-537, 2001)

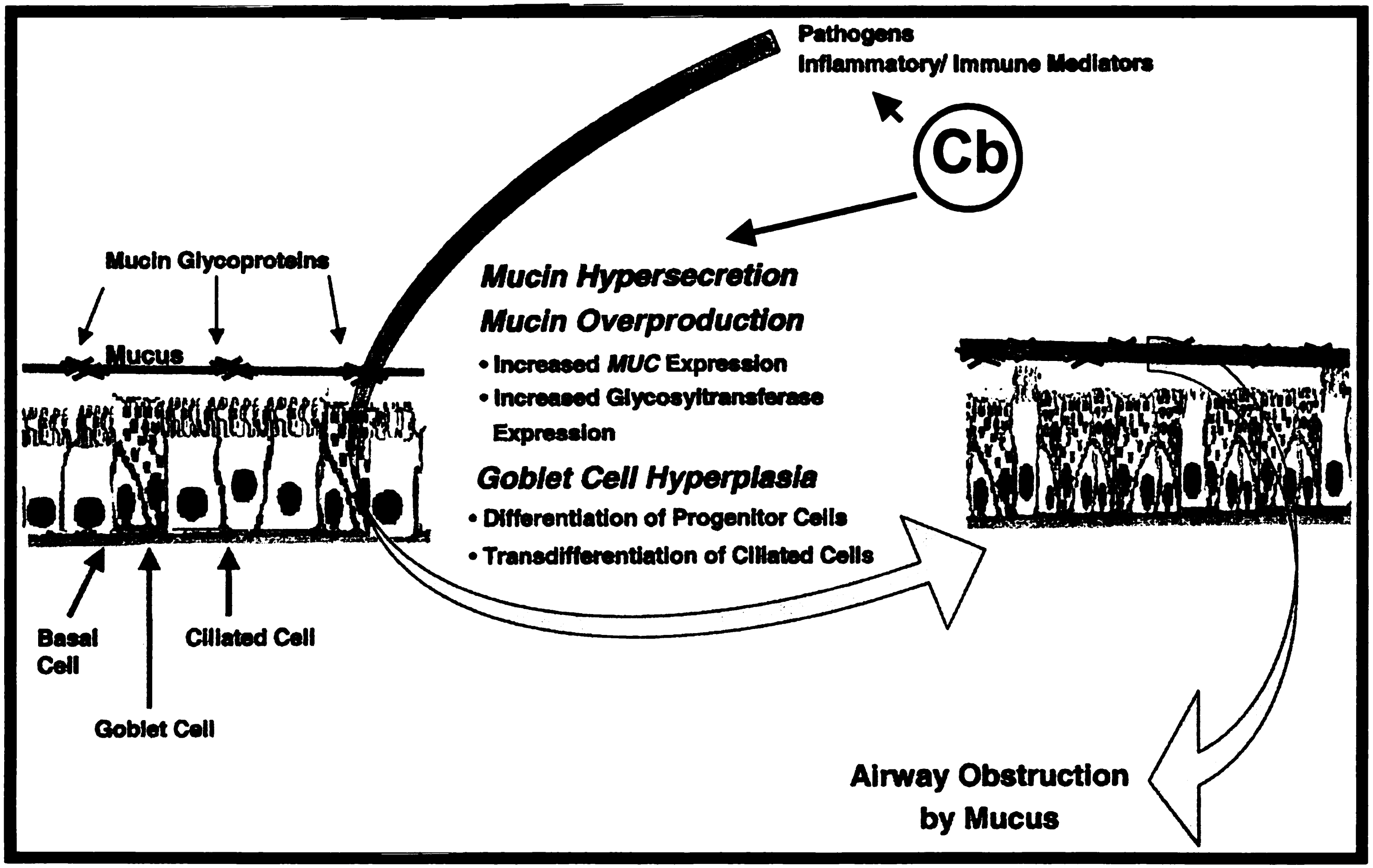

appears to be somehow related to a large surface area on the particles, but its mechanism is not well understood [59, 78].

C. Summary

Particulate compounds are common respiratory tract irritants. Many particle types are known to cause adverse effects in the pulmonary airways of exposed animals and humans, including PM. Particulate matter, a major component of air pollution, has been shown to induce inflammation and oxidative stress in vivo in animal lungs and in vitro in human pulmonary cells. Poorly soluble ultrafine particles are another particle type known to have toxic effects in the pulmonary tissues of exposed animals and humans. Lab rodents chronically exposed to high levels of PSPs such as diesel exhaust particles and titanium dioxide develop inflammation, epithelial alterations, and neoplasia. Particle parameters such as size and surface area have been shown to influence the severity of the pulmonary toxicity of PSPs. The mechanism of PSP toxicity in pulmonary tissues is thought to be by oxidative stress, induced via inflammatory mediators or direct generation of reactive oxygen species.

III. The Nasal Airways

A. Anatomy and Physiology

Aside from olfaction, the nose functions to humidify, warm, and filter inhaled air. Many nasal toxicants can inhibit these normal functions and cause other injury to the nasal mucosa. Epithelial cells lining the airways of the nose are the primary target of injury of inhaled toxicants.

The nasal mucosa of laboratory rodents consists of four types of overlying epithelium: squamous, transitional, respiratory, and olfactory (Figure 3). Stratified squamous epithelium (SE) is composed of basal cells and several layers of squamous cells. Squamous epithelium is a region of high cell proliferation, but is not a sensitive region to inhaled toxicants. Nasal transitional epithelium (NTE) consists of nonciliated cuboidal epithelium 1-2 cell layers thick with no mucous secretory cells. The lack of cilia and mucous cells may make this epithelial type particularly susceptible to injury from inhaled toxicants. Respiratory epithelium (RE) is pseudostratified low-columnar and ciliated, containing various numbers of ciliated cells, mucous cells, and basal cells. In regions of RE, the mucous lining the epithelial layer may protect the nasal airway from inhaled toxicants. Mucociliary clearance is a protective mechanism in the nasal passages, in which inhaled contaminants are trapped in the mucous layer and then removed by cilia-generated mucous flow. Finally, olfactory epithelium (OE) consists of basal, olfactory sensory, and sustentacular cells. Olfactory epithelium plays a vital role in olfaction and xenobiotic metabolism.

Figure 3: Distribution of Rat Nasal Epithelium; Rodents have four types of nasal epithelium: squamous, transitional, respiratory, and olfactory epithelium

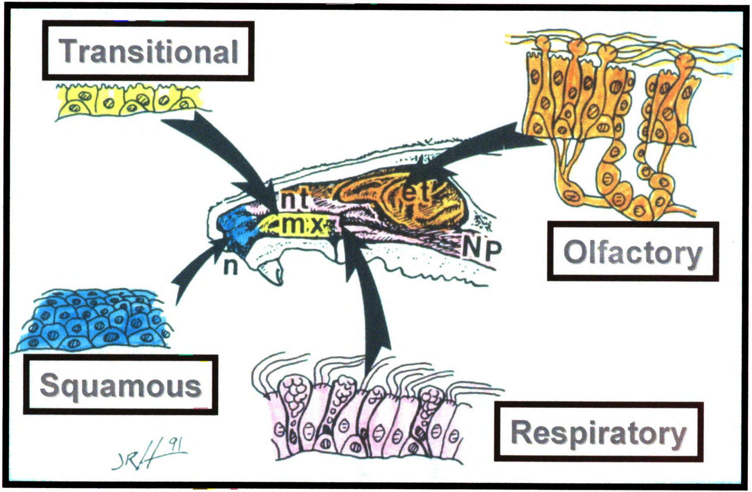

B. Susceptibility to Toxicity

Mucous Cell Metaplasia

A common pathologic feature of nasal toxicity is increased mucus production in epithelial cells and increased numbers of mucous goblet cells in the nasal epithelium in regions that normally have few or no mucous cells present. This change in cell type from non-secretory cell to mucous cell is known as mucous cell metaplasia (MCM). The mechanism by which increased mucus production and mucous metaplasia occur in nasal and pulmonary airways is unknown. Similar and dissimilar pathways may be involved in the development of MCM in response to different stimuli, such as allergens, pathogens, and air pollutants. In rats exposed to an allergen, eosinophils, T-helper 2 (Th2) lymphocytes, and mast cells have been associated with the induction of pulmonary MCM [86]. Specifically, the allergic inflammatory pathways involve stimulation of Th2 and mast cells to produce cytokines such as IL-4, IL-9, and IL-13 [85]. These interleukins appear to increase expression of mucin genes [87]. In contrast to the allergic MCM, rats exposed to stimuli such as ozone and bacterial endotoxin have been reported to induce MCM by a mechanism partly dependent on neutrophilic inflammation and neutrophil-derived products [84]. Exposure to non-allergic pulmonary toxicants leads to the activation of neutrophils to produce elastase and reactive oxygen species, both of which are also known to increase expression of mucin genes [84].

Common pathways for both allergic and non-allergic MCM may exist, wherein EGF receptor activation leads to increases in stored mucous product by way of increased mucin gene expression as well as differentiation of non-secretory cells into mucous goblet cells [88]. Both increased gene expression and cell differentiation are thought to contribute to the pathophysiologic metaplastic response in pulmonary epithelium. Presumably similar mechanisms are involved in the induction of MCM in the nasal airways of rodents exposed to inhaled toxicants and biogenic substances such as allergens and endotoxins.

Gases

It has been well established that the nasal passages are a site for absorption of many gases [89-91]. Several studies have demonstrated susceptibility of the nasal mucosa to injury induced by inhaled gases such as ozone, formaldehyde, and sulfur dioxide [92-94].

Ozone

Ozone (O_3), the main oxidant air pollutant found in smog, has been reported to cause injury to nasal tissues in lab animals and humans. Several studies have investigated the effects of absorbed ozone on rat noses. In either acute (7 days) or chronic (20 months) exposures to 0.5-1.0 ppm O_3 the pulmonary airways of exposed rats exhibited inflammation, by increases in neutrophils and eosinophils, greater DNA synthesis in epithelial cells, epithelial necrosis, exfoliation, secretory hyperplasia and metaplasia, increases in intraepithelial mucosubstances, and bony atrophy [95-99]. Bonnet monkeys exposed to 0.3 ppm O_3 for 90 days had inflammation, epithelial damage, and proliferative and secretory epithelial responses in their nasal mucosae [100, 101]. Finally, in controlled human studies, where subjects were exposed to either air or 0.4-0.5 ppm O_3, ozone was shown to induce moderate epithelial disruption and inflammation in the nasal mucosa of exposed individuals [102-104].

Formaldehyde

Formaldehyde is a well established nasal toxicant and human nasal carcinogen. More than 90% of inhaled formaldehyde gas is absorbed in the upper respiratory tract in rats and monkeys [105]. Rats chronically exposed by inhalation to formaldehyde have been shown to develop squamous-cell carcinomas in the nasal cavities, while acute exposure to the gas appears to mainly increase cell turnover rates in nasal epithelium [106, 107]. Rats and monkeys both get DNA-protein crosslinking in the nasal mucosa upon exposure to formaldehyde, and additionally rats can get point mutations in tumor suppressor genes [108-110]. Other genotoxic lesions include single-strand DNA breaks and chromosomal aberrations in vitro with exposure to the gas [111].

Other Gases

Other gaseous nasal toxicants include sulfur dioxide, hydrogen sulfide, and chlorine gas. Absorption of these gases in the nasal mucosa has varying effects, depending on the type of gas. While sulfur dioxide and hydrogen sulfide target olfactory epithelium, chlorine gas appears to induce epithelial damage throughout the nasal passages [94, 112, 113].

Particles

According to the regional patterns of deposition described in Figure 1, the nasal passages are also a potential target site for particle deposition and injury. Many studies have reported on particle deposition in the nose of lab animals and humans [114-118]. Injury to the nasal airways by inhaled particles has been observed in a number of studies.

Wood dust

Wood dust, a particle type known to be a nasal carcinogen, deposits in the upper and lower airways of humans [119]. Although the sizes of occupational wood dust particles is difficult to determine, in animal exposure studies generated wood dust is about 2-7 μm in size (coarse; [120, 121]). Exposure concentrations can reach higher than 5 mg/m^3, especially in wood furniture and cabinet manufacturing plants [119]. High incidences of adenocarcinomas have been consistently observed in the nasal cavities and sinuses of workers exposed to hardwood dust [120-123]. Many case studies and case-control studies in different occupational groups and regions of the world have shown an increased nasal cancer risk for wood dust workers [121, 122]. The International Agency on Cancer Research has classified hardwood dust as a nasal carcinogen in humans [119].

Diesel Exhaust Particles

Diesel exhaust particles (DEP) have been shown to induce oxidative stress signals (ROS formation) and inflammation (increased inflammatory cytokines) in human nasal epithelial cells in vitro [114, 124]. These epithelial cells were also observed phagocytizing the particles in vitro [114]. An in vivo study involving exposure of guinea pigs to 3.20 mg/m^3 DEP reported enhanced mucosal reactivity and an influx of eosinophils in the nasal mucosa of exposed animals [125]. A nasal cytology study of Swiss customs officers chronically exposed to diesel truck emissions revealed chemically induced rhinitis in exposed workers vs indoor officers [126]. While the rhinitis consisted of substantial goblet cell hyperplasia and metaplasia, as well as increased numbers of leukocytes, the lesions did not appear to be progressive.

Talc

Another type of particle reported to cause nasal injury is nonasbestoform talc. A National Toxicology Program (NTP) lifetime study of rats exposed to 0, 6, or 18 mg/m^3 coarse talc particles showed hyperplasia of nasal respiratory epithelium and the appearance of "eosinophilic droplets" in the epithelium of exposed rats [127]. A second NTP study using a similar exposure regimen with mice found that the same droplets appeared in mouse nasal epithelium in a dose-dependent manner [127].

Particulate Matter

Particulate matter, found in air pollution, has also been implicated in the development of nasal lesions. A series of studies conducted in Metro Mexico City revealed chronic airway injury in children living in the Metro area [128-131]. Epithelial damage in the nasal mucosa of affected children, as evidenced by nasal biopsy, included basal cell hyperplasia, squamous metaplasia, neutrophilic infiltrations, and signs of oxidative DNA damage [128, 131]. Additionally, particulate matter was found inside epithelial cells and in intraepithelial spaces in exposed children [130]. Chronic airway insult, along with DNA damage such as a point mutation in p53 tumor suppressor gene, suggest the eventual possibility of carcinogenic effects in the airways of exposed children [129, 131].

C. Summary

Many gases, vapors, and particles are known to induce adverse effects in the nasal airways of exposed animals and humans. Gases such as ozone and formaldehyde diffuse into the nasal airways of lab animals during exposure, causing nasal lesions including metaplasia, bony atrophy, inflammation, and even nasal tumors. Coarse- and ultrafine-sized particles are also known to deposit in the nasal airways of exposed animals. A few particle types, like wood dust and particulate matter, have been shown to induce nasal inflammation and epithelial alterations in exposed individuals. However, more controlled exposure studies are required in studying the nasal toxicity of particles.

V. Research Goals

Carbon black is an irritant of the respiratory tract. Its ultrafine particle size allows for deposition deep in the pulmonary airways, and many studies have investigated the toxic effects of carbon black particles on the pulmonary airways of animals and humans. Carbon black has been classified as a pulmonary carcinogen in lab rodents. In recent studies, investigators have determined that these ultrafine particles may also deposit in the nasal passages upon exposure. However, no study to date has investigated the adverse effects of carbon black inhalation on the nasal airways. Therefore the guiding hypothesis of the present studies was to determine if long-term inhalation of carbon black particles will cause chronic lesions in the nasal airways of laboratory rodents.

The first hypothesis of this research was that a dose-response relationship would be observed in the nasal mucosa of rodents exposed to carbon black. Rodents exposed to carbon black have indicated an increase in severity of lung lesions with increased concentrations of carbon black exposure [15, 16]. In the case of very high exposure concentrations of carbon black, rodent pulmonary macrophages are known to experience particle burden and clearance of particles becomes inhibited [15, 16]. While moderate concentrations of carbon black induce mild epithelial and inflammatory responses, severe chronic alveolitis and induction of tumorigenic pathways is seen once overload is achieved in the lungs of exposed rats [25]. It is possible that, like in the pulmonary airways, the nasal airways of carbon black-exposed lab rodents will exhibit an increase in severity of lesions with an increase in exposure concentration. In order to answer this question, lab rodents were exposed to low, mid, or high concentrations of carbon black particles, or filtered air alone (no carbon black particles).

The second hypothesis of this research project was that carbon black-induced nasal lesions persist post-exposure. Previous studies have shown that carbon black-induced lung lesions remain in lab rodents for weeks and even months after the end of an exposure period [21, 30]. While the pulmonary responses attenuated given time after exposure, the presence of particles in alveolar macrophages and accompanying inflammation did remain up to two years post-exposure in rodents exposed to chronically to high concentrations of carbon black [21]. Therefore I hypothesized that nasal lesions induced by carbon black may persist for weeks and even months after the end of exposure. To test this hypothesis, rodents in the present study were either sacrificed immediately after the end of exposure, or 13 weeks or 11 months post-exposure.

A third hypothesis tested in the research was that there would be a difference in nasal toxicity depending on the size and surface area of the carbon black particles. Carbon black particles, depending on how they are manufactured and utilized, have different surface area/mass ratios. Smaller sized particles will have a greater surface area than larger sized particles of the same mass when they form airborne spherical aggregates. Therefore, agglomerates of smaller particles have a greater surface area/mass ratio than agglomerates of larger particles. It has been shown that the severity of carbon black-induced pulmonary lesions is dependent on the surface area of the carbon black particles used in the exposure, where particles with higher surface area (smaller in size) had a more adverse effect on pulmonary tissues than did low surface area particles [132]. In the present study rats, which were anticipated to be the most sensitive rodent species to carbon black-induced nasal toxicity, were additionally exposed to a high concentration a low surface area carbon black particle.

Lastly, the research project examined the hypothesis that the severity, persistence, and dose-response of carbon black-induced nasal injury were dependent on the rodent species. Therefore, rats, mice, and hamsters were exposed to one of the three concentrations of carbon black particles, or filtered air alone. I hypothesized that there would be a difference among the three rodent species in carbon black-induced adverse effects.

In summary, the results of the present research project provide an extensive morphologic characterization of carbon black-induced nasal toxicity in three commonly used rodent species. The study provides an examination of the effects of dose, time, particle type, and rodent species on the severity and persistence of carbon black-induced nasal lesions. The implications of the research presented in this study can be related to the human risk to carbon black inhalation exposure. Also the research may provide a starting point for further investigation along the lines of site-specific nasal dosimetry and computer modeling of nasal airflow patterns.

CHAPTER 2

Epithelial and Inflammatory Responses in the Nasal Airways of Rats Chronically Exposed to Carbon Black Particles

I. Introduction

Many inhalation studies have examined the toxicity of carbon black particles to the pulmonary airways [15, 16], but the adverse effects of carbon black on the nasal airways have not been previously investigated. In the previous lung studies, rats were shown to be the most sensitive laboratory rodent species to carbon black toxicity [15, 16]. Additionally, it has been shown that the severity of carbon black-induced pulmonary lesions is dependent on the surface area of the carbon black particles used in the exposure [132]. Therefore, the present study was designed to characterize the morphologic alterations caused by carbon black particles of two different surface areas (high and low) on rat nasal mucosa. It tested the hypothesis that chronic exposure to carbon black particles induce lesions in the nasal airways of laboratory rats.

II. Materials and Methods

Animals

Ninety female Fischer 344 rats (Harlan Sprague-Dawley, Indianapolis, IN), obtained at 5 weeks of age, were used in this study (n=6). The rats were allowed at least two weeks to acclimate before the start of exposures, and were fed Purina rodent chow and water on an *ad libitum* basis throughout the study.

Exposure Protocols

Exposures were conducted under the supervision of Dr. Gunter Oberdorster at the University of Rochester-NY. Rats were exposed in compartmentalized, horizontal flow whole-body inhalation chambers (~300L) to either high surface area carbon black particles (HSCb; Printex 90) or low surface area carbon black particles (LSCb; Sterling V). The HSCb aerosols had a primary particle size of 17 nm and an aerodynamic diameter of 1.4 μm (geometric standard deviation; GSD=2.7); particle surface area was 300 m^2/g. The LSCb aerosols had a primary particle size of 70 nm and an aerodynamic diameter of 0.9 μm (GSD=3.0); particle surface area was 37 m^2/g. The HSCb (Printex 90) was obtained from Degussa-Huels (Germany) and the LSCb (Sterling V) was supplied by Cabot (Boston, MA). Rats were exposed to 0, 1, 7, 50 mg/m^3 HSCb or 50 mg/m^3 LSCb for 6 hours/day, 5 days/week for 13 weeks. Rats were sacrificed 1 day, 13 weeks, or 11 months after the last day of exposure (Figure 4). Images in this thesis are presented in color.

Figure 4: Timeline of Animal Exposure and Sacrifices; Animals were exposed 6 hours/day, 5 days/week, for 13 weeks; Animals were sacrificed either one day, 13 weeks, or 11 months after the end of exposure (PE = post-exposure)

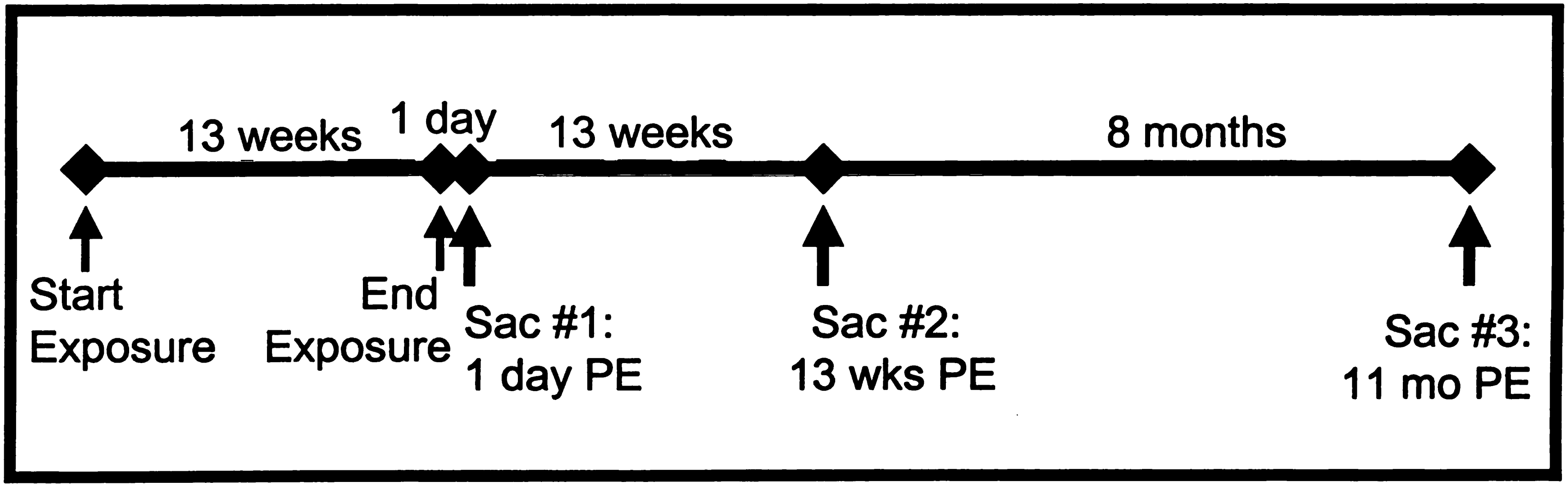

Necropsy and Nasal Tissue Processing

Rats were killed by exsanguination following deep anesthesia induced with 25 mg/kg sodium pentobarbital. Immediately after death, the head of each rat was removed from the carcass, and the eyes, lower jaw, skin, and musculature were removed. The nasal airways of rats were flushed in a retrograde manner through the nasopharyngeal orifice with 2 ml of 10% neutral buffered formalin, and the head was immersed in a large volume of the same fixative for at least 24 hours.

After fixation, heads were decalcified for 7 days in 13% formic acid, and then rinsed in dH_2O for 1-2 hours. After decalcification, the nasal airways were transversely sectioned at four specific anatomic locations, using the following gross dental and palatine landmarks previously described by Young [133]: (*1*) immediately posterior to the upper incisor teeth (tissue block 1); (*2*) at the incisive papilla (tissue block 2); (*3*) at the second palatine ridge (tissue block 3); and (*4*) in the middle of the front upper molar tooth (tissue block 4) (Figure 5). The tissue blocks were embedded in paraffin and 5-µm-thick sections were cut from the anterior face of each block. Nasal tissue sections were histochemically stained with the Alcian blue (pH 2.5)/periodic acid-Schiff stain sequence (AB/PAS) to identify acidic and neutral mucosubstances, or hematoxylin and eosin (H&E) for histopathologic examination. Finally, tissues were stained with a polyclonal anti-rat neutrophil antibody to identify neutrophils located in the airway surface epithelium and lamina propria within the nasal mucosa [134].

Figure 5: Transverse Sections of Rat Nasal Airways Selected for Analysis; Tissue sections T1-T4 (S = septum; NT = nasoturbinate; MT = maxilloturbinate; MS = maxillary sinus; ET = ethmoturbinates; D = nasolacrimal duct; T = root of incisor tooth; B = Brain; NP = nasopharyngeal meatus; HP = hard palate; EY = Eye)

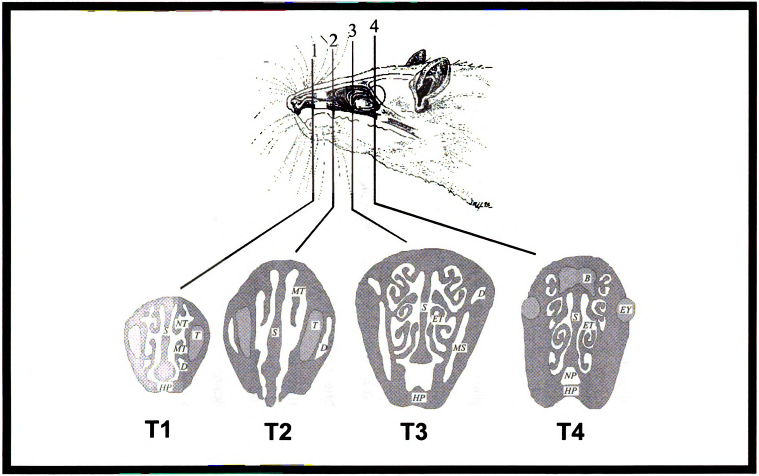

Morphometry

Epithelium covering the maxilloturbinates in sections from tissue block 1 (T1), the midseptum from tissue block 2 (T2), the maxillary sinuses from tissue block 3 (T3), and the floor of the nasopharyngeal meatus from tissue block 4 (T4) were morphometrically analyzed. The medial and lateral surfaces of the maxilloturbinates in the T1 region are covered by nonciliated cuboidal nasal transitional epithelium (NTE) 1-2 cell layers thick with no mucous secretory cells. The epithelium lining the midseptum in the T2 region a columnar ciliated RE with few if any mucous cells. The maxillary sinuses of T3 are lined by pseudostratified tall-columnar RE composed of ciliated, serous, and basal cells. Finally, the floor of the nasopharyngeal meatus of the T4 region is lined by tall-columnar ciliated RE with numerous mucous cells.

The average lengths of epithelium evaluated in each region were 4.6 mm in the maxilloturbinates of T1, 3.7 mm in the T2 septum, 49.1 mm in T3, and 1.7 mm in the T4 region. Morphometric analyses were performed with a semiautomatic, computerized image analysis system consisting of a light microscope (Olympus BX-60; Olympus Corp., Lake Success, NY) connected to a high-resolution CCD camera (e.g., VE-1000; Dage-MTI, Inc., Michigan City, IN), a Scion LG-3 digital image-processing board (Scion Corp., Frederick, MD), a color monitor, and a Dell Dimension XPS T600, running a public-domain image analysis program (NIH Image; written by Wayne Rasband at the U.S. National Institutes of Health). Morphometric techniques were used to determine volume density of intraepithelial mucosubstances, total epithelial cell density, and neutrophil cell density. Detailed descriptions of each technique are given below.

Intraepithelial Mucosubstances (Stored IM)

For each rat, the volume density (Vs) of acidic and neutral (AB/ PAS-positive) intraepithelial mucosubstances (IM) within the surface epithelium overlying the chosen regions in T1-T4 was determined (Figure 6). The areas of AB/ PAS-positive IM were calculated from the automatically circumscribed perimeter of the stained material, and basal lamina lengths were also measured. The method used to mathematically convert these areas and lengths to Vs involved the following formula, originally described in Harkema, et al. [101]:

$$\text{Vs (in nL)} = \frac{\text{Area of mucosubstances (in mm}^2\text{)}}{\text{Length of basal lamina (in mm)} \times 4/\pi} \times 1000$$

Data were expressed as the mean volume density (Vs, in nl/mm^2 basal lamina) of AB/PAS-positive mucosubstances within the epithelium ± SEM.

Epithelial Cell Density

Numeric density of the surface epithelial cells (i.e., epithelial cells/mm basal lamina) was determined by counting the total number of epithelial cell nuclear profiles present in the surface epithelium lining the maxilloturbinates of tissue block T1, and dividing by the total length of the basal lamina underlying the

Figure 6: Intranasal Distribution of HSCb-induced Mucous Cell Metaplasia/Hyperplasia in the Nasal Epithelium of Rats Chronically Exposed to Carbon Black (X and • = location of MCM, • = region chosen for quantitative analysis of MCM)

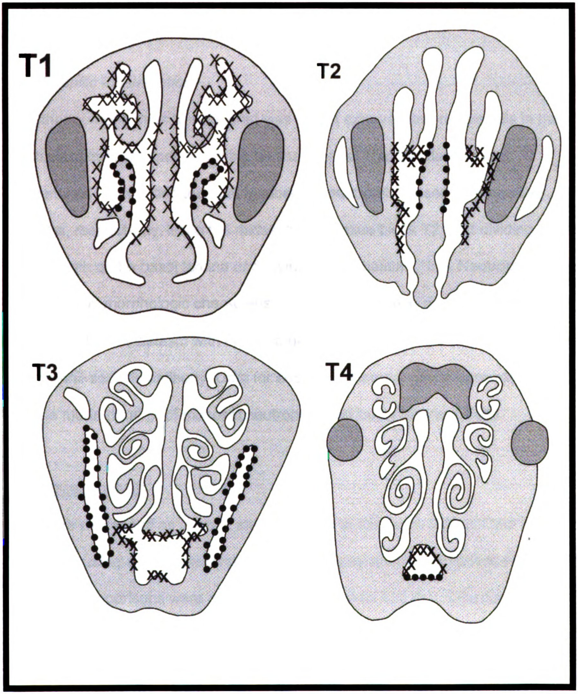

epithelium [135]. Secretory mucous cells were also counted in this epithelium, and expressed as a percentage of total epithelial cells. Data for each experimental group were expressed as the mean number of NTE cells/mm basal lamina ± SEM.

Neutrophilic Inflammation

Another numeric density measured was that of extravasated neutrophils in the surface epithelium and underlying lamina propria. This cell density was determined by counting the total number of neutrophils present in these two regions, respectively, lining the midseptum of tissue block T2, and dividing by the total length of the basal lamina underlying the epithelium [135]. Neutrophils were identified by morphologic characteristics (size, multi-lobed darkly-stained nucleus, clear cytoplasm with dust-like granules) and by positive reactivity to the neutrophil-specific antibody. Data for each experimental group were expressed as the mean number of mucosal neutrophils/mm basal lamina ± SEM.

Statistical Analysis

Data are expressed as mean ± standard error of the mean (SEM). Data were analyzed using a completely randomized two-way analysis of variance (ANOVA). Multiple comparisons were made by the Tukey *post hoc* test. Criterion for significance was taken to be $p \leq 0.05$.

III. Results

Histopathology

At the end of the 13-week exposure, rats exposed to 50 mg/m^3 HSCb had marked morphologic alterations in the surface epithelium and underlying lamina propria lining both the proximal and distal nasal airways (T1-T4). Lesions were present in the nasal tissue lining the medial and lateral meatuses in tissue blocks 1 and 2, in the respiratory epithelium lining the maxillary sinuses and ethmoturbinates in tissue block 3, and in the epithelium lining the nasopharyngeal meatus from tissue block 4 (see Figure 6). The most prominent of these bilateral lesions were found in surface epithelium and underlying lamina propria lining the maxilloturbinates (T1), midseptum (T2), maxillary sinuses (T3), and floor of the nasopharyngeal meatus (T4; see Figure 6).

Tissue Section 1 (T1)

At one day post-exposure (PE), alterations to the nasal epithelium lining tissue section 1 of rats exposed to HSCb were limited to the nasoturbinates, maxilloturbinates, proximal septum, and lateral wall. Carbon black particles were microscopically evident in the nasal mucosa (nasal particle burden) in rats exposed to 50 mg/m^3 HSCb, in the proximal septum, nasoturbinates, and maxilloturbinates. Although no necrosis or cell proliferation were noted in exposed rats, epithelial changes in the maxilloturbinates (T1) included thickening of the NTE due to increased size and numbers of epithelial cells (i.e., epithelial cell hypertrophy and hyperplasia, respectively; Figure 7) and MCM (appearance

Figure 7: HSCb-Induced Epithelial Cell Hyperplasia in Nasal Transitional Epithelium (NTE) Lining Maxilloturbinates of Rats; Light photomicrographs of the maxilloturbinate (T1), stained with H&E, from rats chronically exposed to filtered air (0 mg/m^3) (A), 50 mg/m^3 HSCb (B) for 13 weeks and sacrificed 1 day PE (e = surface epithelium, tb = turbinate bone, bv = blood vessels in lamina propria; arrows = AB/PAS-stained mucosubstances; bar = 50 µm)

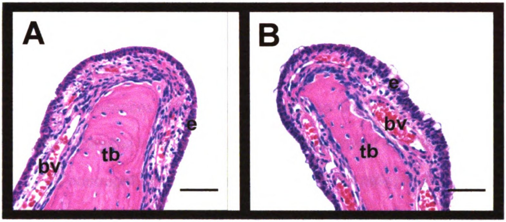

Figure 8: HSCb-Induced Mucous Cell Metaplasia in Transitional Epithelium Lining Maxilloturbinates of Rats; Light photomicrographs of the maxilloturbinate (T1), stained with AB/PAS, from rats chronically exposed to filtered air (0 mg/m^3) (A), 50 mg/m^3 HSCb (B) or 50 mg/m^3 LSCb (C) for 13 weeks and sacrificed 1 day PE (e = surface epithelium, tb = turbinate bone, bv = blood vessels in lamina propria; arrows = AB/PAS-stained mucosubstances; bar = 50 µm)

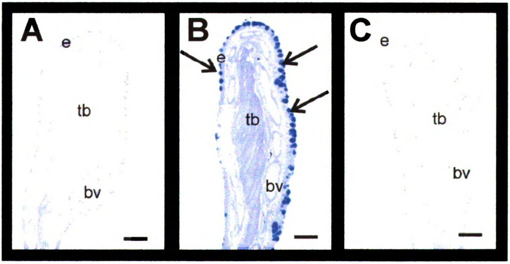

of mucous goblet cells in regions normally containing no or few mucous cells; Figure 8). Air-exposed control rats (0 mg/m^3) had 1- to 2-cell thick nonciliated cuboidal epithelium lacking mucous cells lining their maxilloturbinates, while rats exposed to 50 mg/m^3 HSCb had a metaplastic NTE that was 4- to 6-cell thick nonciliated columnar epithelium with numerous mucous cells. Mucous goblet cells were identified by intracytoplasmic acidic (AB-staining) and neutral (PAS-staining) mucosubstances. Other exposure-induced lesions seen at one day PE in the maxilloturbinates included a mild to moderate mixed inflammatory cell influx (mainly neutrophils and lymphocytes with plasma cells) and mild atrophy of the turbinate bone (Figure 8). Neutrophils were present in varying numbers in the lamina propria underlying the NTE lining the maxilloturbinates of rats exposed to 50 mg/m^3 HSCb. Associated with the neutrophilic inflammation (rhinitis) in the surrounding lamina propria was atrophy of the bone in the dorsal aspect of the maxilloturbinates. Rats exposed to 1 mg/m^3 HSCb or 50 mg/m^3 LSCb did not have any alterations in the NTE lining the maxillotubinates (Figure 8).

At 13 weeks post-exposure, rats exposed to 50 mg/m^3 HSCb had similar but attenuated nasal lesions in the NTE lining the maxillturbinates. Particles in the nasal mucosa of the proximal septum, maxilloturbinates, and nasoturbinates were still present in rats exposed to 50 mg/m^3 HSCb at this time point, at a severity similar to rats similarly exposed and sacrificed one day PE. Nasal inflammation and bony atrophy of the turbinates had resolved by 13 weeks PE in rats exposed to 50 mg/m^3 HSCb. A mild MCM was still present in the NTE lining the maxilloturbinates in these rats, but the metaplasia was significantly reduced compared to similarly exposed rats at one day PE. Carbon black-induced hyperplasia of the NTE was also attenuated but still present at 13 weeks PE.

By 11 months post-exposure, most of the nasal lesions in the maxilloturbinates had resolved in the rats exposed to 50 mg/m^3 HSCb. The only persistent alterations in these rats were a mild MCM and light burden of particles in the nasal tissues of the septum and maxilloturbinates.

Tissue Section 2 (T2)

Alterations in tissue section 2 of rats exposed to HSCb were primarily in the nasal mucosa lining the lateral wall, ethmoid turbinates, and midseptum at one day PE. Carbon black particle burden was substantial in the nasal mucosa at the dorsal part of the midseptum and the ethmoid turbinates in rats exposed to 50 mg/m^3 HSCb. The most conspicuous lesion in this tissue section was a chronic active rhinitis with marked MCM and a mixed inflammatory cell influx (mainly neutrophils with some lymphocytes and plasma cells) in the midseptum of rats exposed to 50 mg/m^3 HSCb (Figure 9). Metaplasia of the respiratory epithelium (RE) lining the midseptum of rats exposed to 7 and 50 mg/m^3 HSCb was characterized by a change in surface epithelium from 1 to 2-cell ciliated low-columnar epithelium with no mucous cells to 4-6 cell ciliated tall-columnar epithelium with many mucous goblet cells present (Figure 9). Additionally, rats exposed to 50 mg/m^3 HSCb had a marked neutrophil infiltration in the epithelium and underlying lamina propria of the midseptum (Figure 10). No epithelial

Figure 9: HSCb-Induced Mucous Cell Metaplasia in Respiratory Epithelium Lining the Midseptum of Rats; Light photomicrographs of the midseptum (T2), stained with H&E (A, C) or AB/PAS (B, D), from rats chronically exposed to filtered air (0 mg/m^3) (A, B), 50 mg/m^3 HSCb (C, D) for 13 weeks and sacrificed 1 day PE (* = mixed inflammatory cell infiltrate in lamina propria; e = surface epithelium, g = glands in lamina propria; arrows = AB/PAS-stained mucosubstances; bar = 25 or 50 μm, as indicated)

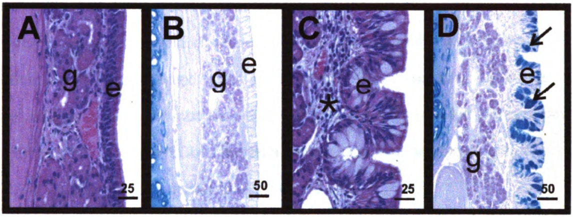

Figure 10: HSCb-Induced Neutrophilic Inflammation in Nasal Mucosa Lining Midseptum of Rats; Light photomicrographs of the midseptum (T2), stained with a neutrophil antibody, from rats chronically exposed to filtered air (0 mg/m^3) (A), 50 mg/m^3 HSCb (B) for 13 weeks and sacrificed 1 day PE (* = mixed inflammatory cell infiltrate in lamina propria; e = surface epithelium, g = glands in lamina propria; n = nerve bundles; arrows = AB/PAS-stained mucosubstances; bar = 50 μm)

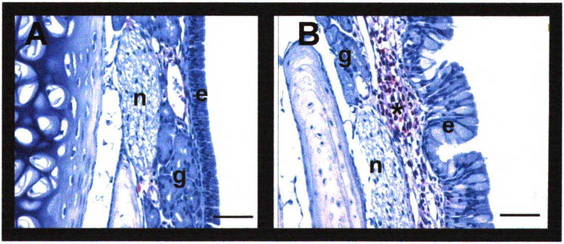

changes were observed in rats exposed to either 1 mg/m^3 HSCb or 50 mg/m^3 LSCb.

While the nasal inflammation (rhinitis) had attenuated by 13 weeks PE in rats exposed to 50 mg/m^3 HSCb, a mild MCM still remained present in the RE lining the midseptum of these rats. However, the amount of stained mucosubstances in the RE at 13 weeks PE was considerably less than the abundant staining observed in rats at 1 day PE. Extensive particle burden was still present in the nasal mucosa of the midseptum and ethmoid turbinates of rats exposed to 50 mg/m^3 HSCb at this time point. In addition, rats exposed to 7 mg/m^3 HSCb had resolved MCM by 13 weeks PE.

By 11 months PE, no nasal lesions were microscopically evident in the T2 section of exposed rats and these rats were histologically similar to those of air-exposed control animals. Only moderate particle burden was present in this tissue section at 11 months PE, in rats exposed to 50 mg/m^3 HSCb.

Tissue Section 3 (T3)

Exposure-induced alterations were also present at 1 day PE in the more distal tissue section 3. Particles were abundant in the nasal associated lymphoid tissue (NALT) of rats exposed to 50 mg/m^3 LSCb, while only mild particle burden was seen in the NALT of rats exposed to HSCb. In the RE lining the maxillary sinuses of air-exposed control rats, the surface epithelium was ciliated low-columnar with no mucous cells present. Rats exposed to 1 mg/m^3 HSCb and 50 mg/m^3 LSCb had no histologically detectable nasal lesions (rhinitis or epithelial alterations).

While rats exposed to 7 and 50 mg/m^3 HSCb showed no loss of cilia or changes in cell number or thickness as compared to air-control animals, they did have a conspicuous MCM in the RE lining the maxillary sinuses (Figure 11).

Rats exposed to 50 mg/m^3 HSCb had a persistent but attenuated MCM in the RE lining the maxillary sinuses at 13 weeks PE. At this time point, rats exposed to 50 mg/m^3 LSCb had heavy particle burden in the NALT, similar to rats exposed to LSCb and sacrificed 1 day PE. By 11 months PE, MCM was still detectable in these rats, but was further attenuated compared to similarly exposed rats sacrificed at 13 weeks PE. Also, rats exposed to 50 mg/m^3 LSCb still had moderate particle burden in the NALT at 11 months PE.

Tissue Section 4 (T4)

Finally, alterations were observed in the most distal section (T4) of the nasal cavity at one day PE. Moderate particle burden was present in the nasal mucosa of the scrolls of the ethmoturbinates of rats exposed to 50 mg/m^3 HSCb. In addition, carbon black-induced alterations were present in the RE lining the nasopharyngeal meatus. Control rats had ciliated columnar RE with some mucous cells lining the floor of the nasopharyngeal meatus. In contrast, rats exposed to 7 and 50 mg/m^3 HSCb showed an increase in the number of AB/PAS-stained mucous cells (i.e., mucous cell hyperplasia; MCH) in this region (Figure 12). Rats exposed to 1 mg/m^3 HSCb and 50 mg/m^3 LSCb had no MCH in the RE of this region, and resembled control animals.

Figure 11: HSCb-Induced Mucous Cell Metaplasia in Respiratory Epithelium Lining the Maxillary Sinuses of Rats; Light photomicrographs of the maxillary sinus (T3), stained with AB/PAS, from rats chronically exposed to filtered air (0 mg/m^3) (A) or 50 mg/m^3 HSCb (B) for 13 weeks and sacrificed 1 day PE (e = surface epithelium; g = Steno's glands in lamina propria; L = lumen of maxillary sinus; arrows = AB/PAS-stained mucosubstances; bar = 50 μm)

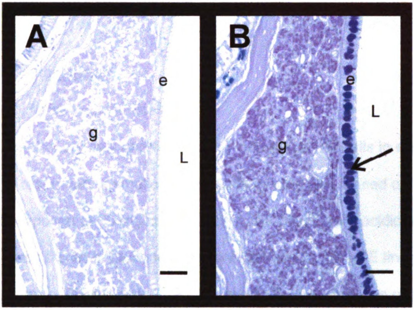

Figure 12: HSCb-Induced Mucous Cell Hyperplasia in Respiratory Epithelium Lining the Floor of the Nasopharyngeal Meatus (NPM) of Rats; Light photomicrographs of the floor of the NPM (T4), stained with AB/PAS, from rats chronically exposed to filtered air (0 mg/m^3) (A), 50 mg/m^3 HSCb (B) for 13 weeks and sacrificed 1 day PE (e = surface epithelium; NPM = Nasopharyngeal meatus; HP= hard palate; arrows = AB/PAS-stained mucosubstances; bar = 50 μm)

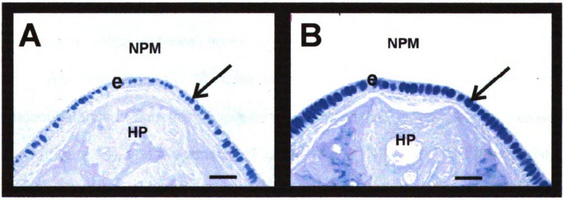

All nasal changes, including particle burden in the ethmoturbinates and MCH in the epithelium lining the nasopharyngeal meatus, had resolved by 13 weeks PE in exposed rats, and remained similar to control rats through 11 months PE.

Morphometric Quantitiation

Stored Intraepithelial Mucosubstances

Air-exposed control animals had no or a few mucous goblet cells in either their transitional or respiratory epithelia. In comparison with air-exposed control animals, rats exposed to 50 mg/m^3 HSCb had 786 times more acidic and neutral mucosubstances stored in mucous secretory cells within the NTE lining the maxilloturbinates in T1 at one day PE (Figure 13). A decrease was observed in the amount of stored mucosubstances in the NTE of rats exposed to 50 mg/m^3 HSCb by thirteen weeks after the end of exposure. By this time, rats previously exposed to 50 mg/m^3 HSCb had 8 times more IM within the NTE as compared to air-controls (90% less than at the end of exposure; Figure 13). At eleven months post-exposure, the NTE lining the maxilloturbinates still had significantly more (16-fold) stored IM than air-control animals (39 times less IM than rats exposed to 50 mg/m^3 HSCb and killed immediately at the end of exposure; Figure 13).

Animals exposed to 50 mg/m^3 HSCb also had 45 times more stored mucosubstances within the RE overlying the midseptum in T2 than rats exposed to air (Figure 14), and this amount of stored IM was reduced by 13 weeks post-

Figure 13: Intraepithelial Mucosubstances in Maxilloturbinates (T1) of Rats Exposed to Carbon Black; * = significantly different from respective control group, □ = significantly different from respective 1 mg/m3 group, • = significantly different from respective 7 mg/m3 group, ▲ = significantly different from respective 50 mg/m3 LSCb group a = significantly different from respective 1 day PE group, b = significantly different from respective 13 weeks PE group, ($p<0.05$)

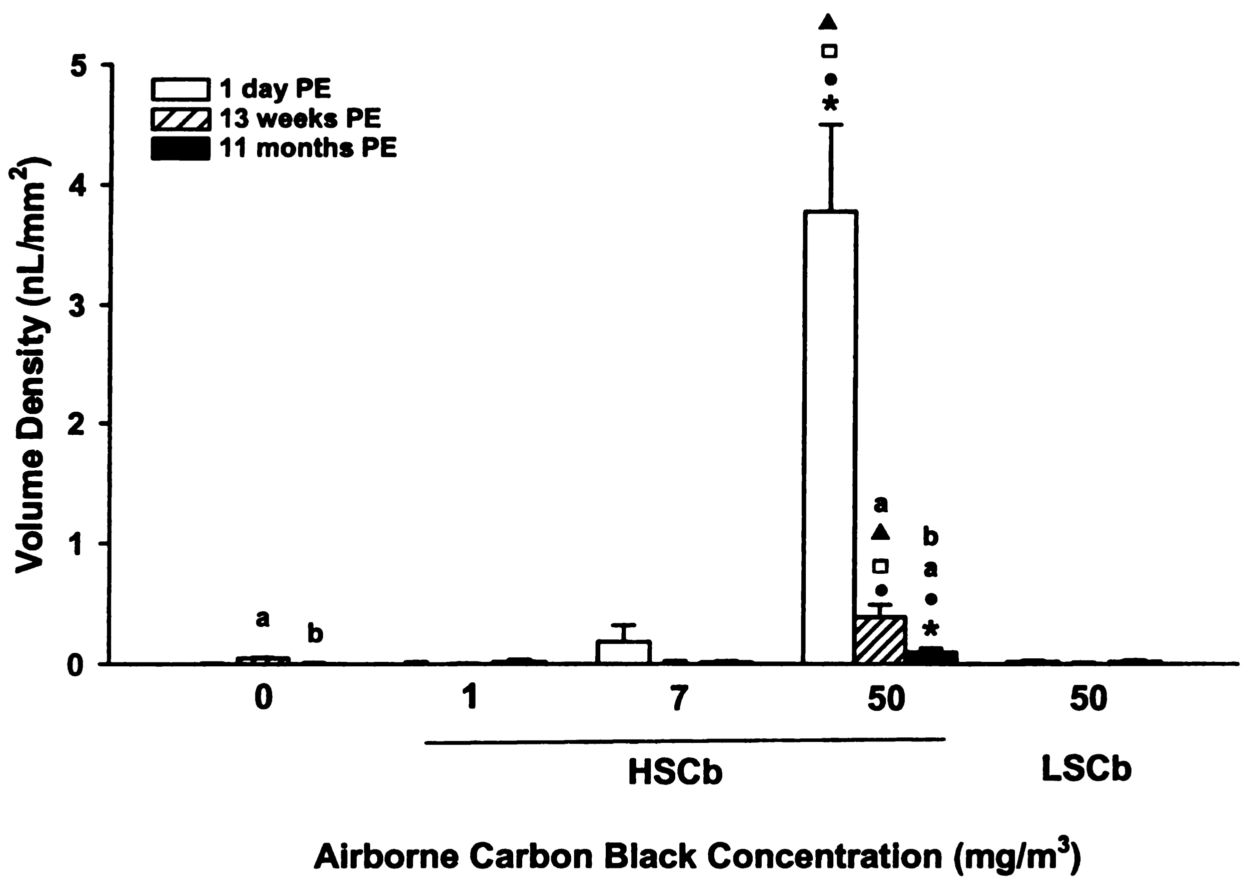

exposure to 11 times more IM than that of air-exposed controls (95% less than at the end of exposure; Figure 14). By eleven months after the end of exposure, the volume density (Vs) of mucosubstances of rats exposed to 50 mg/m^3 HSCb in the RE lining T2 was at a level similar to control animals (Figure 14).

Additionally, significant increases in the Vs of mucosubstances were observed in rats exposed to 50 mg/m^3 HSCb in the RE lining the maxillary sinuses in T3 and the floor of the nasopharyngeal meatus in T4 (Figures 15-16). The increased Vs persisted in the maxillary sinuses, but not in the nasopharyngeal meatus, through 13 weeks post-exposure (Figures 15-16). Even at 11 months after the end of exposure, the RE lining the maxillary sinuses had significantly more (6-fold) stored IM than control animals (14 times less IM than animals exposed to 50 mg/m^3 HSCb and sacrificed immediately at the end of exposure; Figure 15).

Immediately after the end of exposure, a significant Vs of mucosubstances was also found in rats exposed to 7 mg/m^3 HSCb in the RE of selected regions in T2, T3, and T4 (Figures 14-16). Rats exposed to 1 mg/m^3 HSCb or 50 mg/m^3 LSCb showed no change in stored IM in the epithelium lining T1-T4 at any examined time post-exposure (Figures 13-16).

Nasal Epithelial Cell Density

The effects of chronic carbon black particle exposure on the number of epithelial cells in the NTE lining the maxilloturbinates (T1) were determined by quantitating the number of epithelial cell nuclei per millimeter of basal lamina. Rats exposed

Figure 14: Intraepithelial Mucosubstances in Midseptum (T2) of Rats Exposed to Carbon Black; * = significantly different from respective control group, □ = significantly different from respective 1 mg/m3 group, • = significantly different from respective 7 mg/m3 group, ▲ = significantly different from respective 50 mg/m3 LSCb group a = significantly different from respective 1 day PE group, ($p<0.05$); N/D = not detected

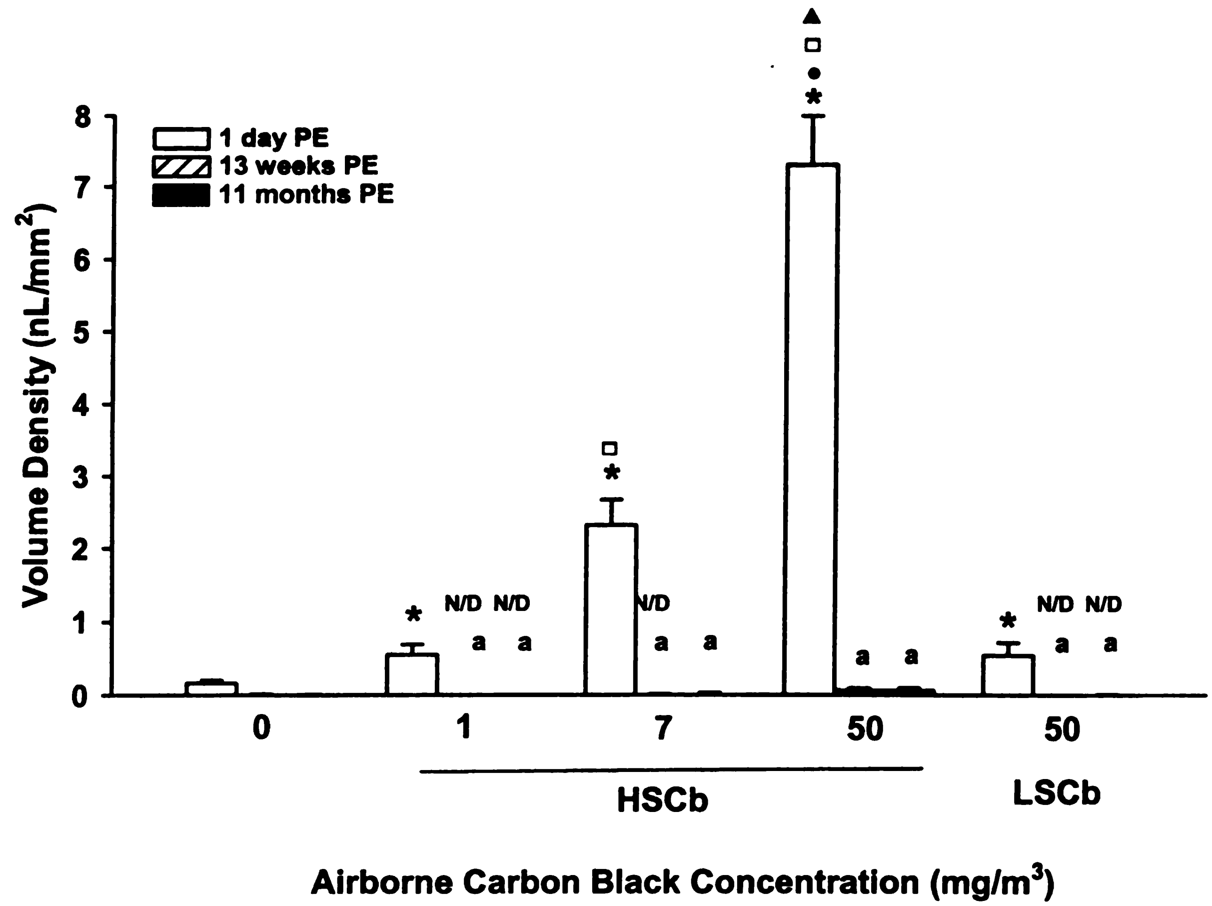

Figure 15: Intraepithelial Mucosubstances in Maxillary Sinuses (T3) of Rats Exposed to Carbon Black; * = significantly different from respective control group, □ = significantly different from respective 1 mg/m3 group, • = significantly different from respective 7 mg/m3 group, ▲ = significantly different from respective 50 mg/m3 LSCb group a = significantly different from respective 1 day PE group, ($p<0.05$); N/D = not detected

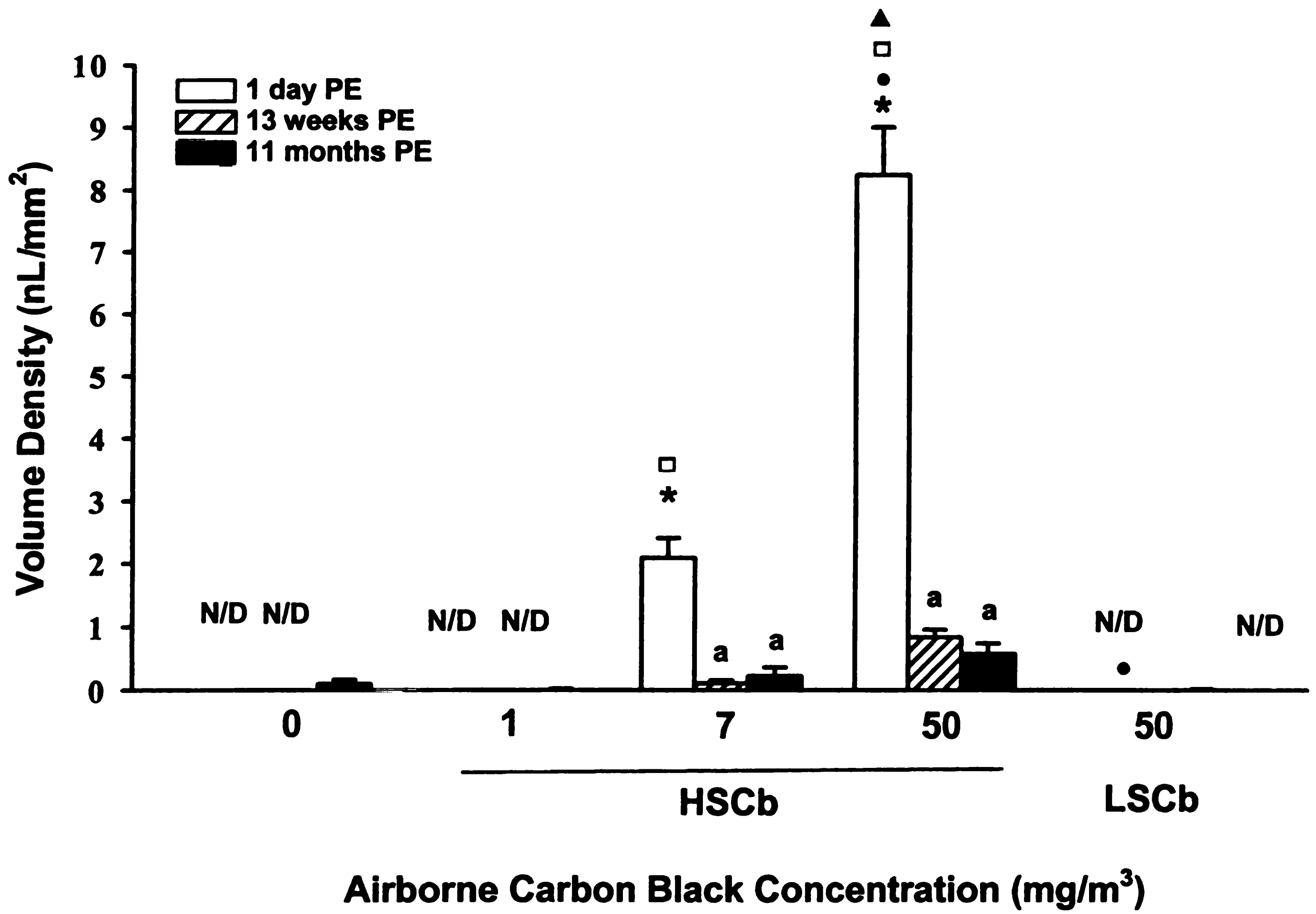

Figure 16: Intraepithelial Mucosubstances in the Floor of the Nasopharyngeal Meatus (T4) of Rats Exposed to Carbon Black; * = significantly different from respective control group, □ = significantly different from respective 1 mg/m3 group, ▲ = significantly different from respective 50 mg/m3 LSCb group a = significantly different from respective 1 day PE group, b = significantly different from respective 13 weeks PE group, ($p<0.05$)

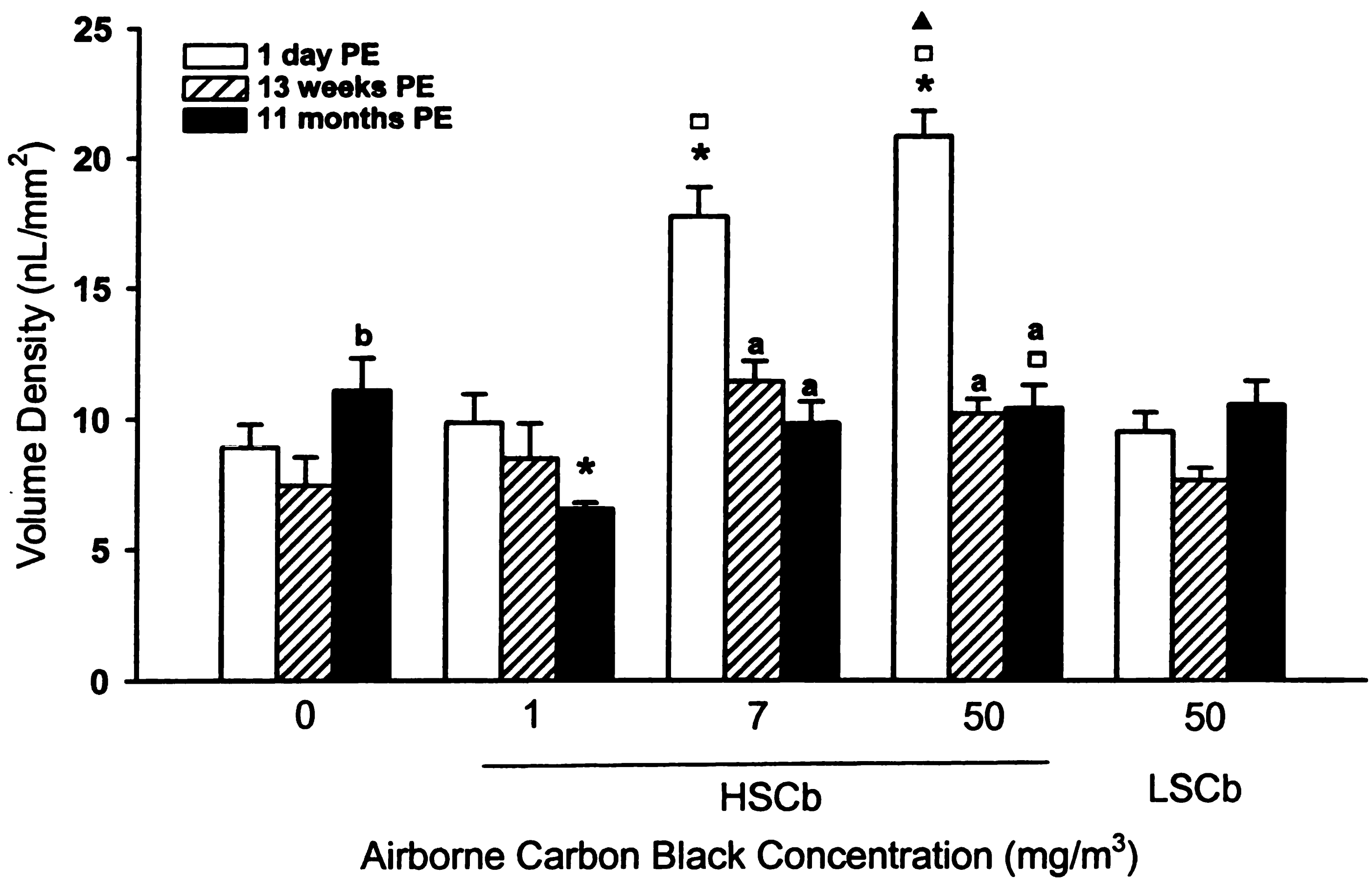

to 50 mg/m^3 HSCb for 13 weeks had significantly more epithelial cells overlying their maxilloturbinates (13% increase) versus air-exposed controls (Figure 17). This increase in epithelial cell numeric density (i.e., epithelial cell hyperplasia) was accompanied by a concomitant increase in the number of AB/PAS-positive mucous secretory cells (see Figure 13) in the surface epithelium. There was no change in the epithelial cell density in the maxilloturbinates of air-exposed control rats or rats exposed to 50 mg/m^3 LSCb (Figure 17).

Increases in total epithelial cells versus air-exposed control animals in the NTE lining the maxilloturbinates persisted to 13 weeks post-exposure in rats exposed to 50 mg/m^3 HSCb (40% increase; Figure 17). This epithelial cell hyperplasia had resolved by 11 months PE, such that total epithelial cell density in the NTE was equivalent to the level of animals exposed only to filtered air (0 mg/m^3 HSCb).

Nasal Inflammation

Neutrophil cell density in the regions lining the maxilloturbinates (NTE; T1) and midseptum (RE; T2) of rats exposed to carbon black particles for 13 weeks was quantified by measuring the number of neutrophils per millimeter basal lamina in the epithelium and lamina propria. Neutrophils were sparse and randomly distributed in the T1 region of rats exposed to air, 50 mg/m^3 HSCb, or 50 mg/m^3 LSCb, with more cells in the lamina propria than in the epithelium (data not shown). Marked inflammation was seen in the T2 region of rats exposed to 50 mg/m^3 HSCb, characterized by a marked increase (6-fold) in the number of cells

Figure 17: Total Epithelial Cell Density in Maxilloturbinates (T1) of Rats Exposed to Carbon Black; * = significantly different from respective control group, ($p<0.05$)

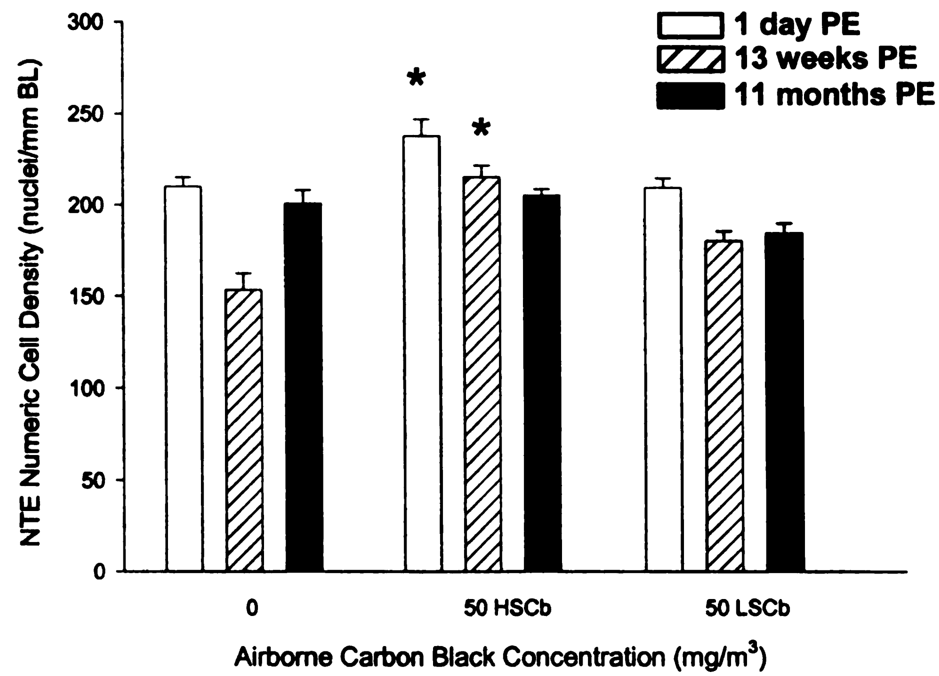

Figure 18: Neutrophils in Nasal Mucosa Lining the Midseptum (T2) of Rats Exposed to Carbon Black; * = significantly different from respective control group, ($p<0.05$)

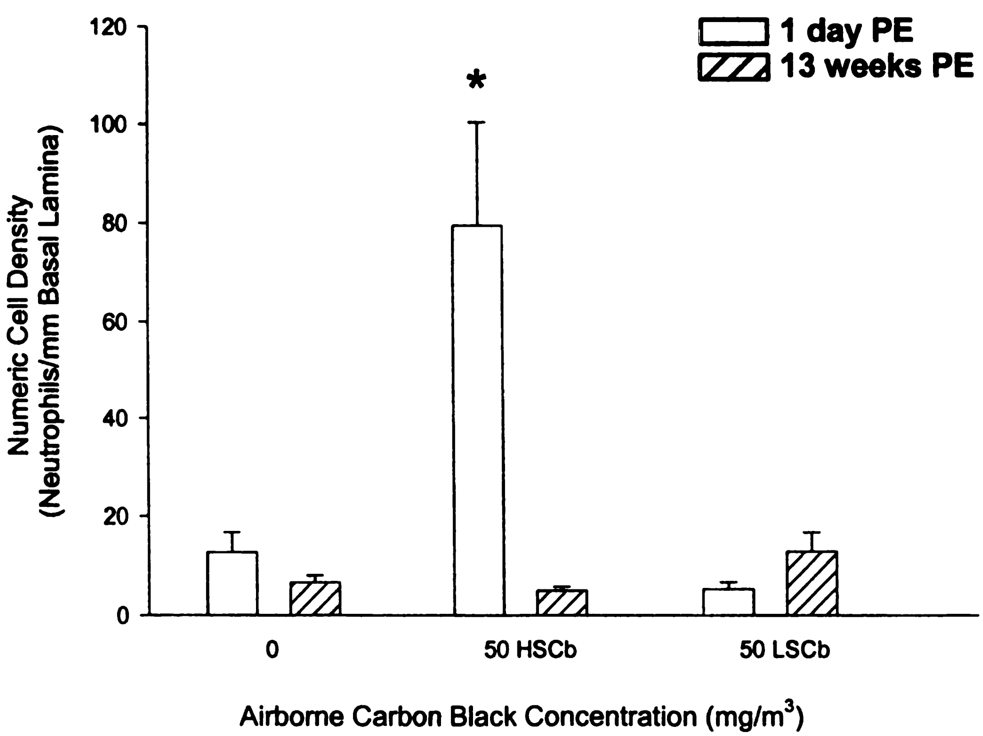

in the epithelium and lamina propria versus air-control animals (Figure 18). No inflammatory response was observed in the T2 region in air-control animals or those exposed to 50 mg/m^3 LSCb (Figure 18).

Thirteen weeks after the end of exposure, the inflammation, characterized by NTE neutrophil cell density, in rats previously exposed to 50 mg/m^3 HSCb had attenuated to control levels, and remained at control levels through 11 months post-exposure.

IV. Discussion

In the present study, I assessed the effects of long-term inhalation of carbon black particles on the nasal airways of rats. I found that the persistence of lesions in the nasal airways of the rats was dependent on time, dose, and particle surface area.

The results of this study indicate that HSCb-induced MCM persists through 11 months after the end of a long-term exposure. A concomitant increase in total epithelial cells (ECH) accompanied the MCM in rats exposed to 50 mg/m^3 HSCb up to 13 weeks post-exposure. In contrast to these persistent lesions, a transient neutrophilic inflammatory response was observed in rats exposed to 50 mg/m^3 HSCb at one day post-exposure, which resolved by 13 weeks post-exposure. Unlike the high concentration of HSCb, 50 mg/m^3 LSCb did not induce alterations in the nasal mucosa of exposed rats.

Some carbon black-induced nasal lesions described in the present study followed a similar pattern of severity as pulmonary lesions found in these same rats [21, 30]. Preliminary data show a dose-dependent relationship in pulmonary lesions in the rats exposed to carbon black particles, which was also seen in nasal lesions as described in the present study. Inflammatory responses in the pulmonary and nasal airways of these rats were restricted to those exposed to the highest concentration of carbon black as well. Unlike the nasal lesions, however, the severity of pulmonary lesions in these rats did not appear to be dependent on time post-exposure or particle surface area.

Many other nasal toxicants, such as vanadium, formaldehyde, sulfur dioxide, and ozone, produce long-lasting lesions in the nasal mucosa of laboratory rodents similar to those induced by carbon black particles observed in the present study [92-94, 136]. In particular, at high concentrations ozone has been shown to induce a persistent MCM and epithelial cell hyperplasia in the maxilloturbinates of rats, not unlike the persistent MCM and ECH that were evident in the HSCb-exposed rats of the present study. In a previous study, rats were exposed to 0, 0.25, or 0.5 ppm ozone for 8 hours/day, 7 days/week, for 13 weeks, and sacrificed 8 hours, 4 weeks, or 13 weeks after the end of exposure [92]. Nasal lesions observed in the study included severe MCM and epithelial hyperplasia in the NTE lining the maxilloturbinates of rats exposed to 0.5 ppm O_3, both of which attenuated but persisted with time post-exposure. Also, a dose-response relationship was observed with the epithelial hyperplastic lesion at 8 hours PE. Morphologically, the nasal lesions in the NTE induced by 50 mg/m^3 HSCb observed in the present study at 1 day PE were very similar to those induced by 0.5 ppm O_3 at 8 hours PE. Nasal pathology common to both the carbon black and ozone exposures included the presence of numerous mucous goblet cells, thickened epithelium, bony atrophy, and inflammatory cell influx. Given the similarity between the two responses, I speculate that some of the cellular and molecular mechanisms responsible for carbon black-induced MCM may be similar to those involved in ozone.

Mechanisms of the MCM induced by ozone in the pulmonary and nasal airways of rats are hypothesized to involve the formation of oxygen free radicals generated from infiltrating neutrophils [84]. Neutrophilic inflammation, as observed in the pulmonary and nasal airways of rats exposed to ozone, is known to play a crucial role in the pathogenesis of MCM. Neutrophils release elastase, a serine protease that impairs mucociliary clearance and stimulates goblet cell metaplasia and mucin production in pulmonary epithelial cells [84]. Neutrophils may also be involved in the generation of reactive oxygen species (ROS) in these pulmonary cells [83]. ROS may in turn enhance intraepithelial mucous synthesis and secretion, as well as upregulate mucin gene expression [84].

Mechanisms of ultrafine particle toxicity in the pulmonary airways of laboratory rodents have also been investigated. Ultrafine particles have been shown to directly induce the formation of reactive oxygen species [59, 78]. It is thought that pulmonary MCM and increased mucin gene expression are induced by these oxygen free radicals. Therefore, I speculate that carbon black-induced nasal lesions occur either via inflammatory mediators (proteases or oxygen free radicals) or by direct particle-induced generation of reactive oxygen species.

The persistent effects of chronic exposure to carbon black particles on either the pulmonary or nasal epithelial cells of humans are unknown. One survey study of carbon black production facility workers suggested that cumulative exposures to carbon black were associated with an increase in chronic bronchitis [11]. However, there has been no study to this date describing significant pathologic effects of carbon black inhalation on the airways of humans. The severity and persistence of carbon black-induced MCM in rats, as shown by the present study, suggest that inhalation of carbon black particles may have the potential to induce similar long-lasting alterations in the nasal airways of humans. The short- and long-term consequences of such an airway alteration to human health are yet to be determined.

CHAPTER 3

Pathology of the Nasal Mucosa of Lab Rodents After a Chronic Carbon Black Exposure: A Species Comparison

I. Introduction

In the previous study I showed that the severity and persistence of nasal lesions induced by carbon black particle (Cb) inhalation exposure is dependent on dose, surface area, and time post-exposure (Chapter 2). The results of the study indicated a dose-response relationship between severity of the nasal lesions and carbon black concentration, greater severity of lesions with high-surface area carbon black (HSCb) than with low-surface area carbon black (LSCb), and persistence of some lesions for several weeks and months post-exposure.

Other laboratory rodents may or may not respond to inhaled carbon black particles in a manner similar to the rats. Previous studies have shown a species difference in pulmonary responses to carbon black inhalation, as well as exposure to many other respiratory toxicants [75, 137-139]. In general these studies have reported that epithelial, inflammatory, and tumorigenic responses in the pulmonary airways were most severe in rats exposed to inhaled toxicants, and less severe in other rodent species such as mice and hamsters [75, 137, 139]. Therefore, the hypothesis of the present study was that there is a difference in nasal toxicity of carbon black among three rodent species: rats, mice, and hamsters.

II. Materials and Methods

Animals

Seventy two female Fischer 344 rats (Harlan; Indianapolis, IN), 72 female $B_6C_3F_1$ mice (Charles River; Wilmington, MA), and 72 female Syrian golden hamsters (BioBreeders; Watertown, MA), all obtained at 5 weeks of age, were used in this study (n=6).

Exposures

Exposures were conducted in the same manner as in the study from Chapter 2. However, in the present study rodents were exposed only to high surface area carbon black particles (HSCb; Printex 90). The HSCb aerosols had a primary particle size of 17 nm and an aerodynamic diameter of 1.4 μm (GSD=2.7); particle surface area was 300 m^2/g. All animals were exposed to 0, 1, 7, or 50 mg/m^3 HSCb for 6 hours/day, 5 days/week for 13 weeks. Rodents were sacrificed 1 day, 13 weeks, or 11 months after the last day of exposure (see Figure 4).

Histologic Analysis

Animal sacrifices and histologic preparation and analysis were all conducted on the rodents using the same technique as described in Chapter 2 (pg. 34-52). Additionally, mice were immunohistochemically stained with an antibody to a chitinase-like protein Ym1/Ym2 found in eosinophilic globules in nasal epithelial cells [140].

Morphometry

Analysis of nasal tissues was conducted using standard morphometric techniques described in Chapter 2. The same measurements were made on the rodents of this study as were made on the rats in the previous study (Chapter 2): volume density of stored intraepithelial mucosubstances, epithelial cell density, and neutrophil cell density.

Statistical Analysis

Data are expressed as mean ± standard error of the mean (SEM). Data were analyzed using a completely randomized two-way analysis of variance (ANOVA). Multiple comparisons were made by the Tukey *post hoc* test. Criterion for significance was taken to be $p \leq 0.05$.

III. Results

Histopathology

Rats

Rats exposed to 50 mg/m^3 HSCb had markedly severe and persistent nasal lesions in the epithelium and underlying lamina propria lining several regions of the nasal cavity. The regions most conspicuously affected were the maxilloturbinates (T1), midseptum (T2), maxillary sinuses (T3), and floor of the nasopharyngeal meatus (T4). The histopathologic description of these lesions included mucous-cell metaplasia/hyperplasia (MCM/MCH), epithelial cell hyperplasia (ECH), and rhinitis (Chapter 2). At one day post-exposure (PE), rats exposed to 7 and 50 mg/m^3 had chronic active rhinitis with MCM and ECH. The lesions appeared to attenuate given time post-exposure (inflammation and hyperplasia), but MCM was still present at 11 months PE in some regions of nasal epithelium in rats exposed to 50 mg/m^3 HSCb (Chapter 2).

Mice

At the end of the 13-week exposure, mice exposed to 50 mg/m^3 HSCb had moderate carbon black particle burden restricted to the nasal mucosa of the midseptum (T2) and NALT (T3). At one day PE mice exposed to 7 and 50 mg/m^3 HSCb also had epithelial changes restricted to the NTE lining the maxilloturbinates (T1) and RE lining the maxillary sinuses (T3). Epithelial metaplasia from a 1-2 cell thick nonciliated cuboidal epithelium lacking mucous cells to a 4-6 cell thick nonciliated columar epithelium with mucous cells was observed in the NTE lining the maxilloturbinates of mice exposed to 7 and 50 mg/m^3 HSCb (Figure 19). Along with this mucous cell metaplasia, mice exposed to 50 mg/m^3 HSCb had an increased thickness in the NTE due to epithelial hyperplasia (i.e., increased numbers of epithelial cells) and epithelial hypertrophy (i.e., increased sizes of epithelial cells; Figure 20). The hypertrophy appeared to be due to hyalinosis of the NTE with intracytoplasmic accumulation of eosinophilic globules in the metaplastic mucous goblet cells (Figure 20). These eosinophilic globules contained a chitinase-like protein Ym1/Ym2, which was immunohistochemically identified using an antibody specific to the protein. Mice exposed to 1 mg/m^3 HSCb had no nasal lesions in the epithelium or underlying submucosa lining the maxilloturbinates.

Mucous cell metaplasia without hyalinosis or Ym1/Ym2 accumulation was also observed in the RE lining the maxillary sinuses of mice exposed to 7 and 50 mg/m^3 HSCb (Figure 21). While air-exposed control animals had a thin ciliated low-columnar RE with no mucous cells present, mice exposed to 7 and 50 mg/m^3 HSCb had moderate staining of mucosubstances in this region of RE. Again, mice exposed to 1 mg/m^3 HSCb had no nasal lesions in the RE lining the maxillary sinuses. Nasal lesions, such as MCM, ECH, and rhinitis, were not observed in any other region of nasal epithelium of exposed mice (Figures 22 and 23).

By 13 weeks PE, the increases in mucosubstances (i.e., MCM) had resolved in all regions of nasal epithelium in mice exposed to HSCb. The only nasal lesion that persisted to 13 weeks PE was the thickened NTE (i.e.,

Figure 19: HSCb-Induced Mucous Cell Metaplasia in Transitional Epithelium Lining Maxilloturbinates of Rats and Mice, but not Hamsters; Light photomicrographs of the maxilloturbinate (T1), stained with AB/PAS, from rats (A, B), mice (C, D), and hamsters (E, F) chronically exposed to filtered air (0 mg/m^3) (A, C, E) or 50 mg/m^3 HSCb (B, D, F) for 13 weeks and sacrificed 1 day PE (e = surface epithelium, tb = turbinate bone, bv = blood vessels in lamina propria; arrows = AB/PAS-stained mucosubstances; bar = 50 µm)

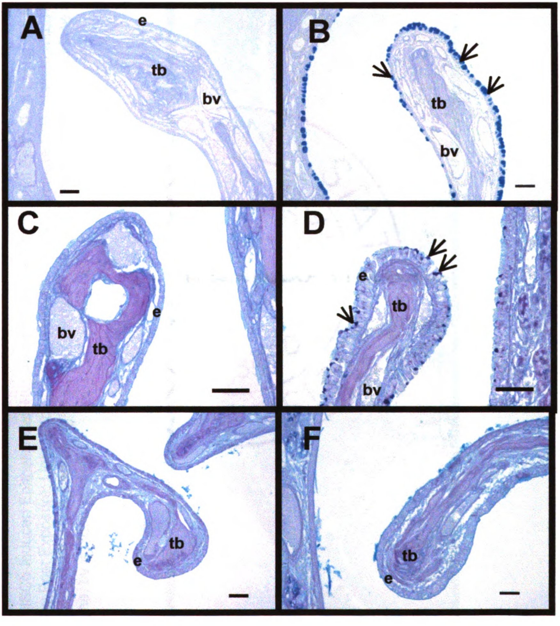

Figure 20: HSCb-Induced Epithelial Cell Hyperplasia in Nasal Transitional Epithelium Lining the Maxilloturbinates of Mice at 1 Day Post Exposure; Light photomicrographs of the maxilloturbinate (T1), stained with H&E, from mice chronically exposed to filtered air (0 mg/m^3) (A) or 50 mg/m^3 HSCb (B) for 13 weeks (e = surface epithelium, tb = turbinate bone, bv = blood vessel)

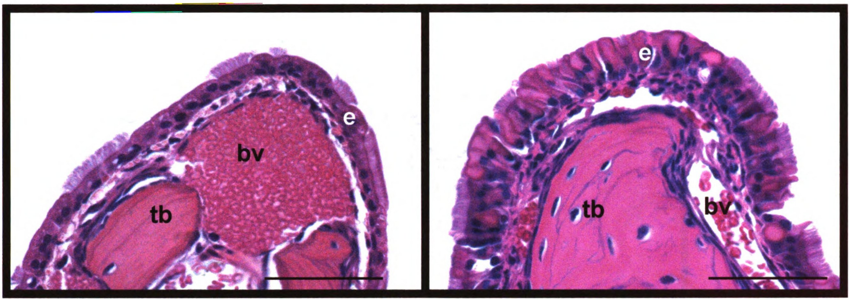

Figure 21: HSCb-Induced Mucous Cell Metaplasia in Respiratory Epithelium Lining the Maxillary Sinuses of Rats and Mice, but not Hamsters; Light photomicrographs of the maxillary sinuses (T3), stained with AB/PAS, from rats (A, B), mice (C, D), and hamsters (E, F) chronically exposed to filtered air (0 mg/m^3) (A, C, E) or 50 mg/m^3 HSCb (B, D, F) for 13 weeks and sacrificed 1 day PE (e = surface epithelium; g = Steno's glands in lamina propria; L = lumen of maxillary sinus; arrows = AB/PAS-stained mucosubstances; bar = 50 μm)

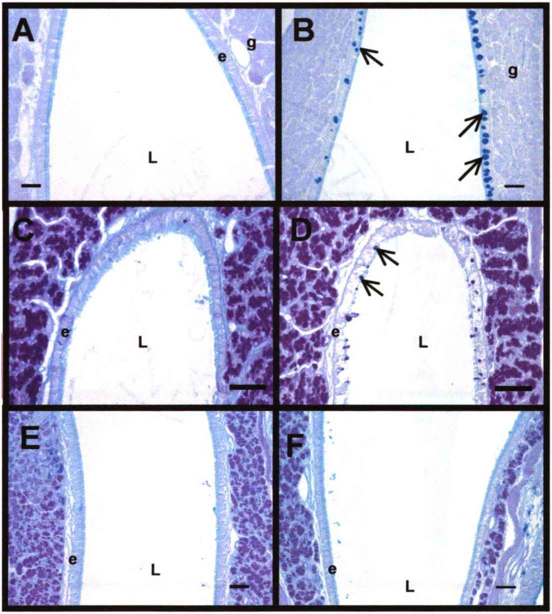

Figure 22: HSCb-Induced Mucous Cell Metaplasia in Respiratory Epithelium Lining Midseptum of Rats, but not Mice and Hamsters; Light photomicrographs of the midseptum (T2), stained with AB/PAS, from rats (A, B), mice (C, D), and hamsters (E, F) chronically exposed to filtered air (0 mg/m^3) (A, C, E) or 50 mg/m^3 HSCb (B, D, F) for 13 weeks and sacrificed 1 day PE (e = surface epithelium, g = glands in lamina propria; arrows = AB/PAS-stained mucosubstances; bar = 50 μm)

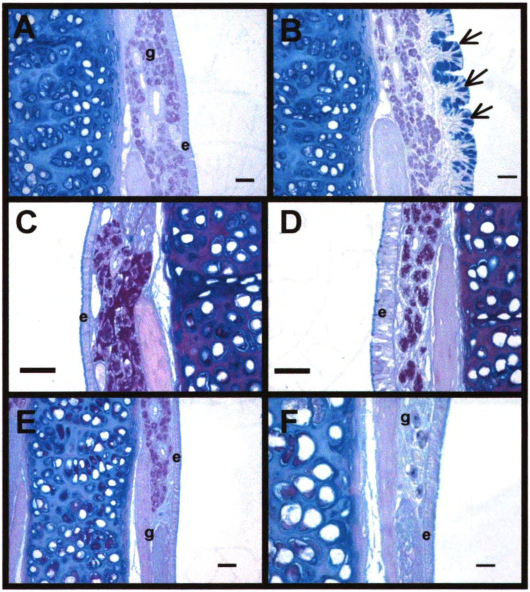

Figure 23: HSCb-Induced Mucous Cell Hyperplasia in Respiratory Epithelium Lining the Floor of the Nasopharyngeal Meatus (NPM) of Rats and Hamsters, but not Mice; Light photomicrographs of the floor of the NPM (T4), stained with AB/PAS, from rats (A, B), mice (C, D), and hamsters (E, F) chronically exposed to filtered air (0 mg/m^3) (A, C, E) or 50 mg/m^3 HSCb (B, D, F) for 13 weeks and sacrificed 1 day PE (e = surface epithelium; NPM = Nasopharyngeal meatus; HP= hard palate; arrows = AB/PAS-stained mucosubstances; bar = 50 μm)

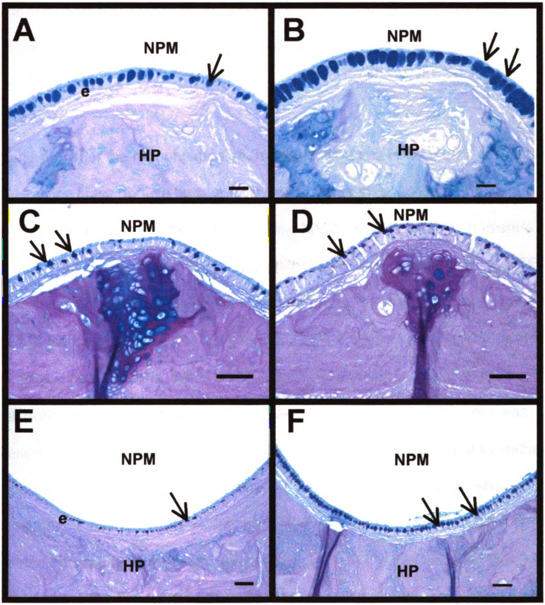

hyperplasia and hypertrophy) lining the maxilloturbinates in mice exposed to 50 mg/m^3 HSCb. The hyerplasia had attenuated from 1 day PE, but the number of cells was still significantly increased compared to air-control mice sacrificed at this time point. Mice exposed to 50 mg/m^3 also still had moderate particle burden in the midseptum and NALT at 13 weeks PE. By 11 months PE, however, mild particle burden was only present in the midseptum, and all nasal epithelial lesions had resolved in the tissues of mice exposed to HSCb.

Hamsters

At one day after the end of exposure, hamsters exposed to 50 mg/m^3 HSCb had mild carbon black particle burden restricted to the nasal mucosa of the maxilloturbinates (T1), midseptum (T2), and NALT (T3). In addition, hamsters exposed to 7 and 50 mg/m^3 HSCb had epithelial alterations limited to the NTE lining the maxilloturbinates and RE lining the floor of the nasopharyngeal meatus (NPM). Hamsters exposed to 1 mg/m^3 HSCb did not have any microscopically detectable nasal lesions. While no MCM was observed in the NTE lining the maxilloturbinates of exposed hamsters, increases in non-secretory cells was present (Figure 24). Mild thickening of the transitional epithelium due to epithelial hyperplasia was observed in hamsters exposed to 50 mg/m^3 HSCb. Also, hamsters exposed to 7 and 50 mg/m^3 HSCb had mild increases in AB/PAS-stained intraepithelial mucosubstances (i.e., mucous cell hyperplasia; MCH) in the RE lining the floor of the NPM (Figure 23). No nasal lesions were observed in any other region of the nasal airways in these exposed hamsters (Figures 19-22).

Figure 24: HSCb-Induced Epithelial Cell Hyperplasia in Nasal Transitional Epithelium Lining the Maxilloturbinates of Hamsters at 1 Day Post Exposure; Light photomicrographs of the maxilloturbinate (T1), stained with H&E, from hamsters chronically exposed to (A) Filtered air (0 mg/m^3) or (B) 50 mg/m^3 HSCb for 13 weeks; e = surface epithelium, tb = turbinate bone, bv = blood vessel

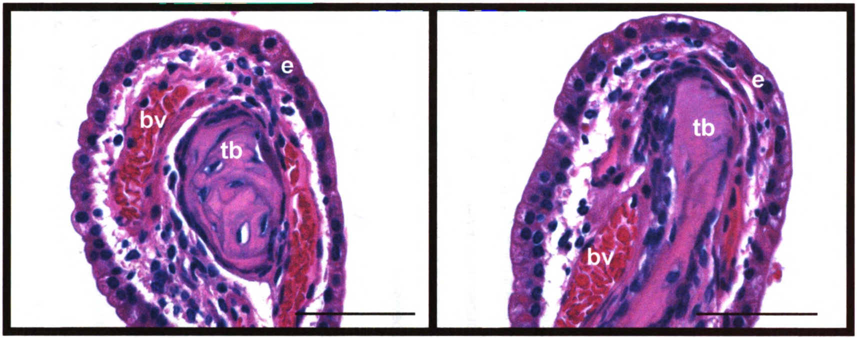

All nasal alterations, including MCH, ECH, and particle burden, had resolved by 13 weeks post-exposure in the exposed hamsters.

Stored Intraepithelial Mucosubstances

Rats

Volume densities of mucosubstances in rats exposed to HSCb have been previously described with figures in Chapter 2 (see Figures 13-16).

Mice

Increases in the volume density (Vs) of stored mucosubstances were observed in mice exposed to 7 and 50 mg/m^3 HSCb in both the NTE lining the T1 maxilloturbinates and the RE lining the T3 maxillary sinuses immediately post-exposure (Figures 25-26). The metaplastic lesions in both of these regions had resolved by 13 weeks post-exposure. No MCM or MCH was observed in the RE lining the T2 midseptum or the T4 floor (Figures 27-28).

Mice exposed to 0 or 1 mg/m^3 HSCb showed no increase in IM in sections T1-T4 (Figures 25-28).

Hamsters

Hamsters exposed to 7 and 50 mg/m^3 HSCb exhibited a mild mucous cell hyperplasia (MCH) in the RE lining the floor of the nasopharyngeal meatus (Figure 28). This hyperplastic response was attenuated by 13 weeks PE, and was the only observable change in intraepithelial mucosubstances in hamsters

Figure 25: Intraepithelial Mucosubstances in the Maxilloturbinates (T1) of Laboratory Animals Exposed to Carbon Black at 1 day PE; * = significantly different from control group within same species, a = significantly different from rats group within same exposure, b = significantly different from mice group within same exposure, ($p<0.05$); N/D = not detected

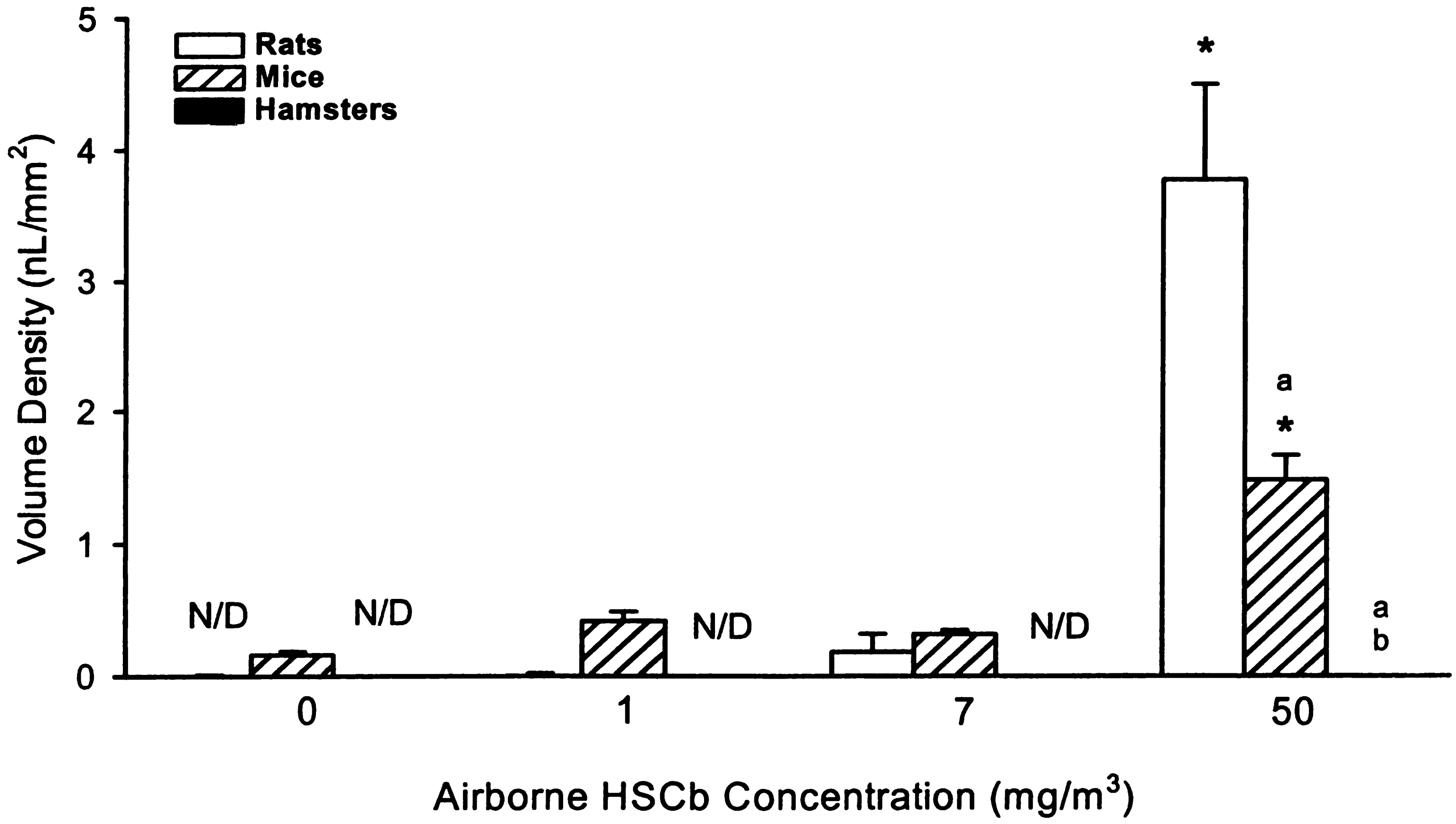

Figure 26: Intraepithelial Mucosubstances in the Maxillary Sinuses (T3) of Laboratory Animals Exposed to Carbon Black at 1 day PE; * = significantly different from control group within same species, a = significantly different from rats group within same exposure, ($p<0.05$); N/D = not detected

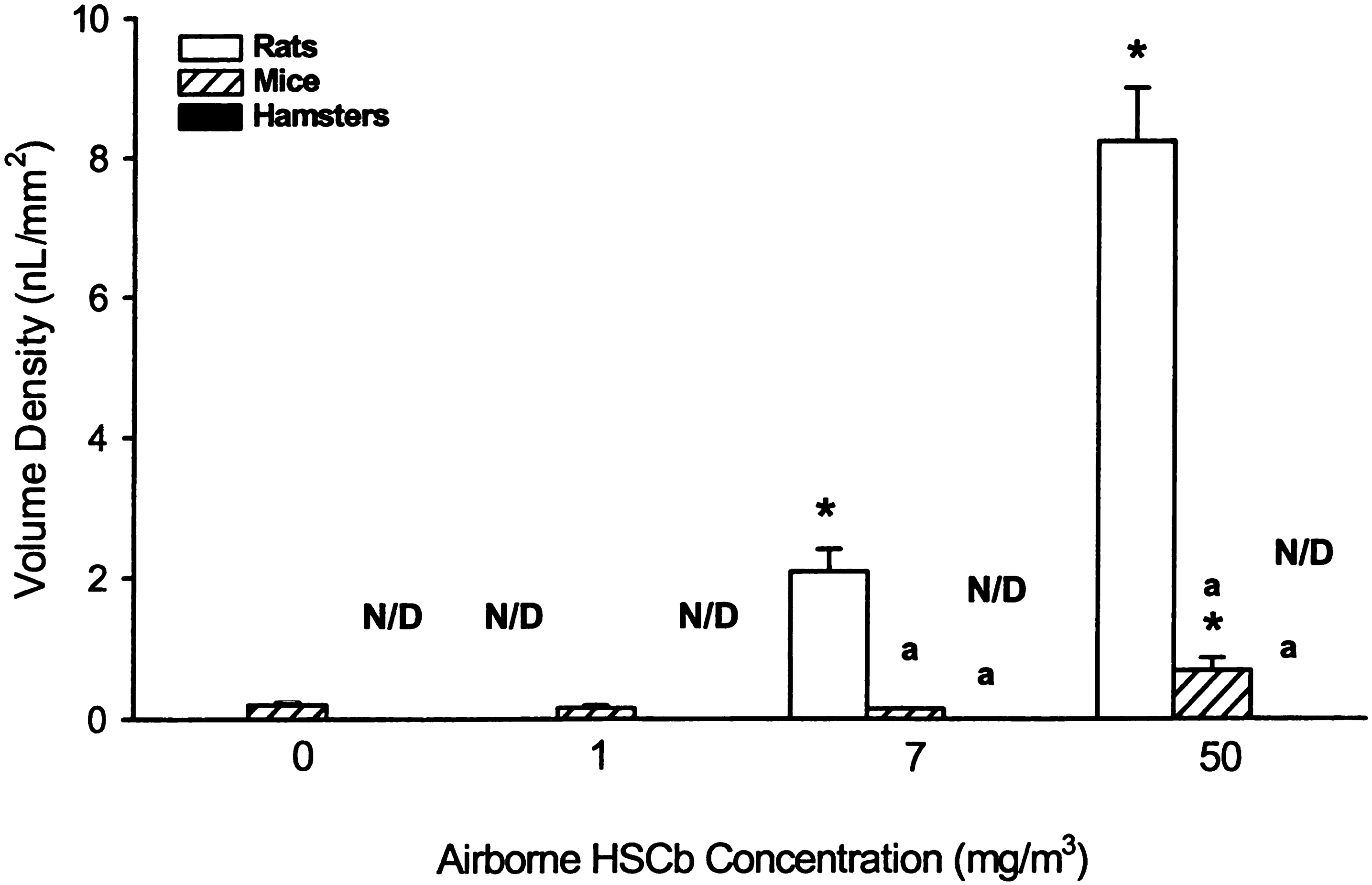

Figure 27: Intraepithelial Mucosubstances in the Midseptum (T2) of Laboratory Animals Exposed to Carbon Black at 1 day PE; * = significantly different from control group within same species, a = significantly different from rats group within same exposure, ($p<0.05$); N/D = not detected

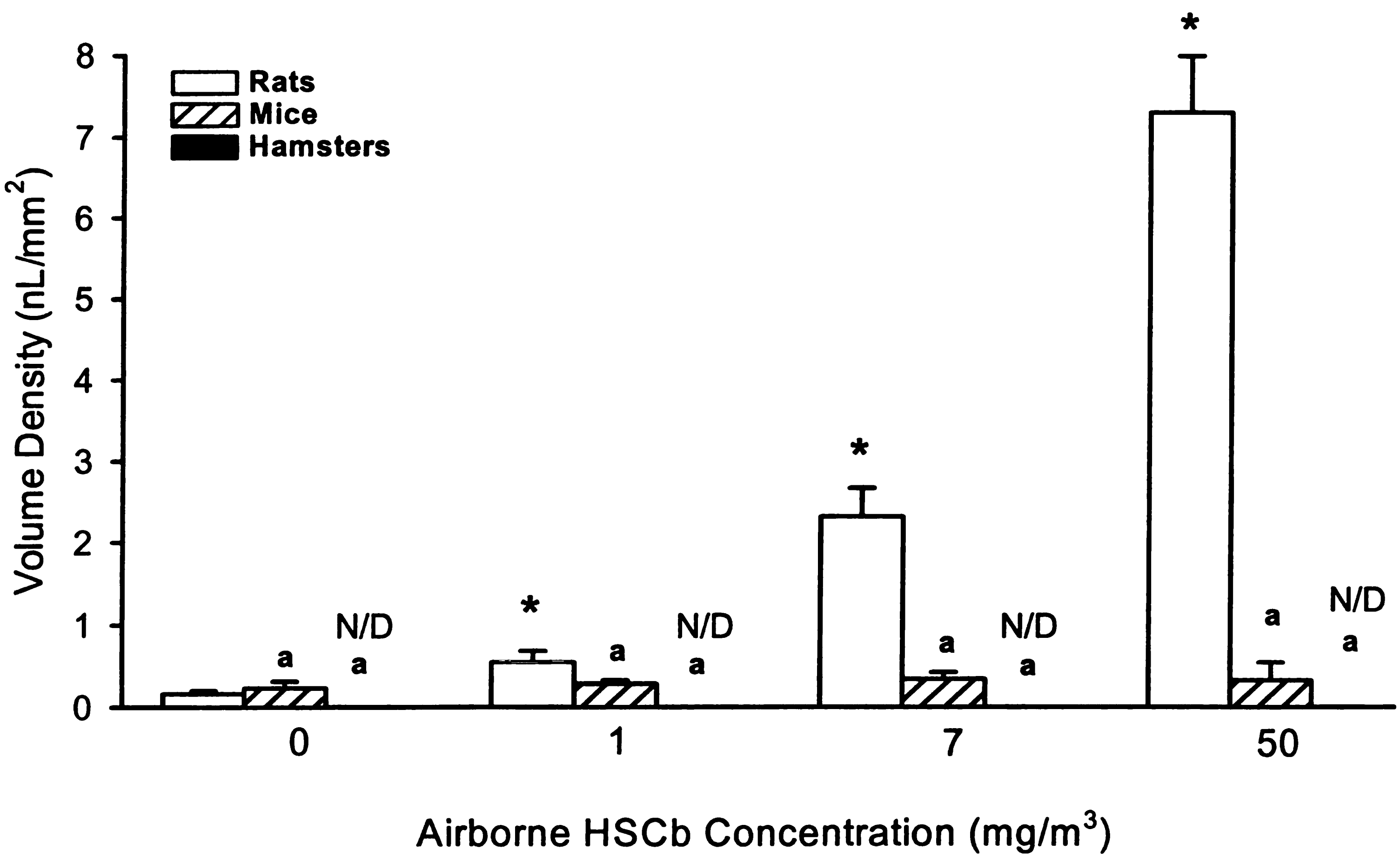

Figure 28: Intraepithelial Mucosubstances in the Floor of the Nasopharyngeal Meatus (T4) of Laboratory Animals Exposed to Carbon Black at 1 day PE; * = significantly different from control group within same species, a = significantly different from rats group within same exposure, b = significantly different from mice group within same exposure, ($p<0.05$)

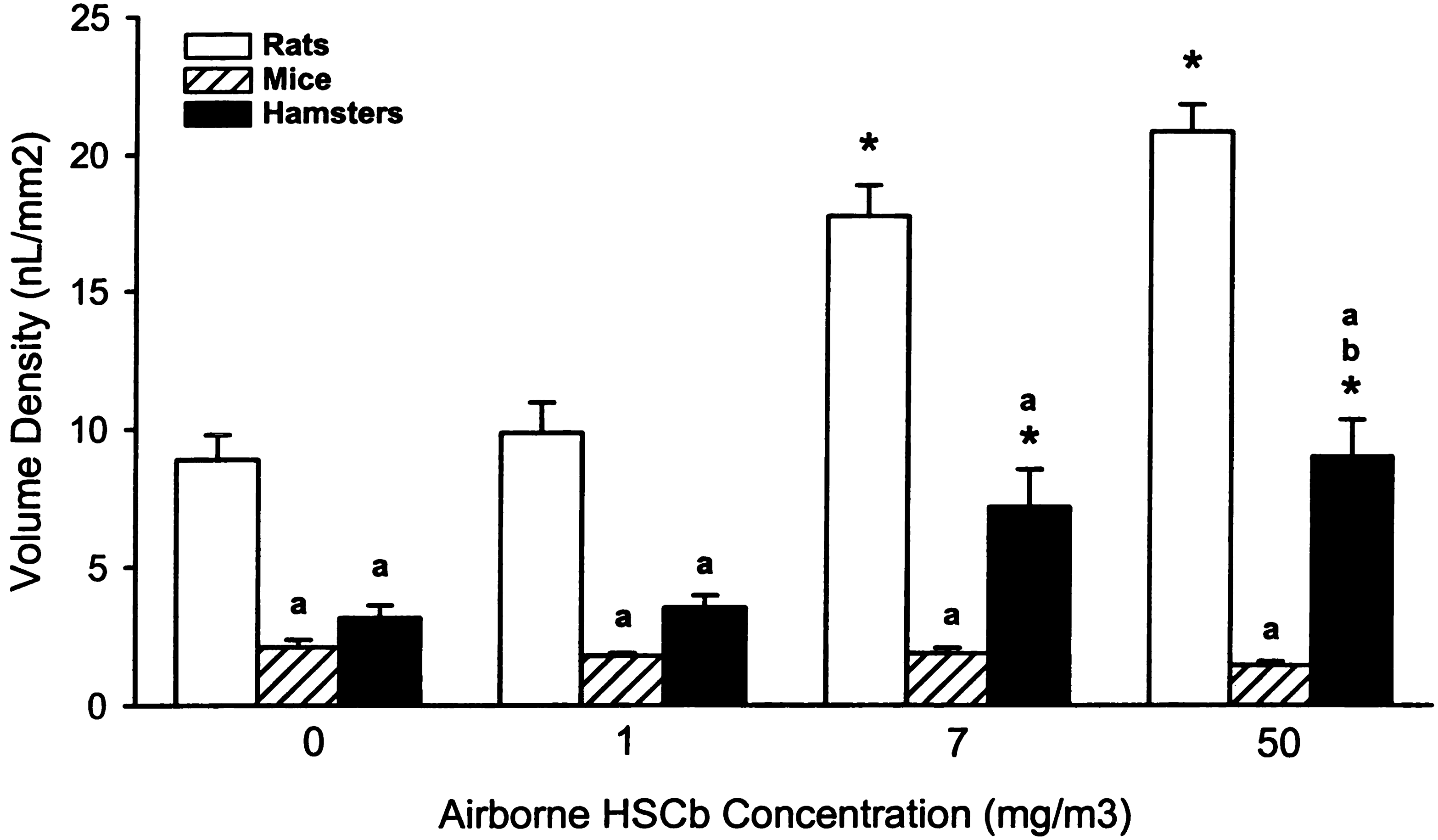

exposed to HSCb. No HSCb-induced increases in the Vs of IM were present in hamsters in any of the other more proximal regions (T1-T3) of the nasal airway and at any exposure concentration or time point PE (Figures 25-27).

Interspecies Comparison

Increases in stored intraepithelial mucosubstances varied in severity and persistence among rats, mice, and hamsters exposed to carbon black particles (Figure 29). MCM was by far most severe and persistent in the NTE and RE lining the nasal airways of rats exposed to HSCb. Mice also had a milder increase in stored IM in some of the same NTE and RE-lined regions, but these increases were much less marked than those observed in rats exposed to similar concentrations of carbon black. At one day post-exposure, rats exposed to 50 mg/m^3 HSCb had approximately 14x, 22x, and 11x more IM in the proximal, middle, and distal parts of the nasal airways, respectively, than mice exposed to the same concentration of HSCb. In these respective areas, hamsters exposed to the same concentration of carbon black had minimal IM. While HSCb-induced lesions persisted in rats until 11 months PE, such lesions in mice and hamsters were resolved by 13 weeks.

Nasal Epithelial Cell Density

Rats

Total epithelial cell densities in rats exposed to HSCb have been previously described with figures in Chapter 2 (see Figure 17).

Figure 29: Species Comparison of the Severity of Mucous Cell Metaplasia in Rats, Mice, and Hamsters Chronically Exposed to 50 mg/m^3 HSCb at One day Post-Exposure (T1-T4 = selected anatomic regions of nasal epithelium in tissue sections 1-4; ↑ = 2x more mucosubstances than respective air-control animals, ↑↑ = 3x more mucosubstances, ↑↑↑ = 4x more mucosubstances, ↑↑↑↑ = 5x more mucosubstances)

	T1	T2	T3	T4
Rat	↑↑	↑↑↑↑	↑↑↑↑	↑↑
Mouse	↑	-	↑	-
Hamster	-	-	-	↑

Mice

Increases in the number of total epithelial cells in the NTE lining the maxillotubinates of mice exposed to 50 mg/m^3 HSCb were present at one day PE as compared to mice exposed to only filtered air (0 mg/m^3 HSCb; Figure 30). This increased epithelial cell density vs. control mice persisted to 13 weeks PE, but resolved by 11 months PE in similarly exposed rats (Figure 30).

Hamsters

Hamsters exposed to 50 mg/m^3 HSCb had a mild increase in total epithelial cell density in the NTE lining the maxilloturbinates at one day PE (Figure 31). By 13 weeks PE, the epithelial cell density had resolved to levels similar to those of air-exposed control hamsters, and remained resolved through 11 months PE (Figure 31).

<u>Nasal Inflammation</u>

Rats

Neutrophil cell densities in rats exposed to HSCb have been previously described with figures in Chapter 2 (see Figure 18).

Mice

Mice exposed to 50 mg/m^3 HSCb had minimal numbers of neutrophils in the epithelium or underlying lamina propria lining the midseptum (T2) at one day

Figure 30: Total Epithelial Cell Density in T1 Maxilloturbinates of Mice Exposed to Carbon Black; * = significantly different from respective control group, ($p<0.05$)

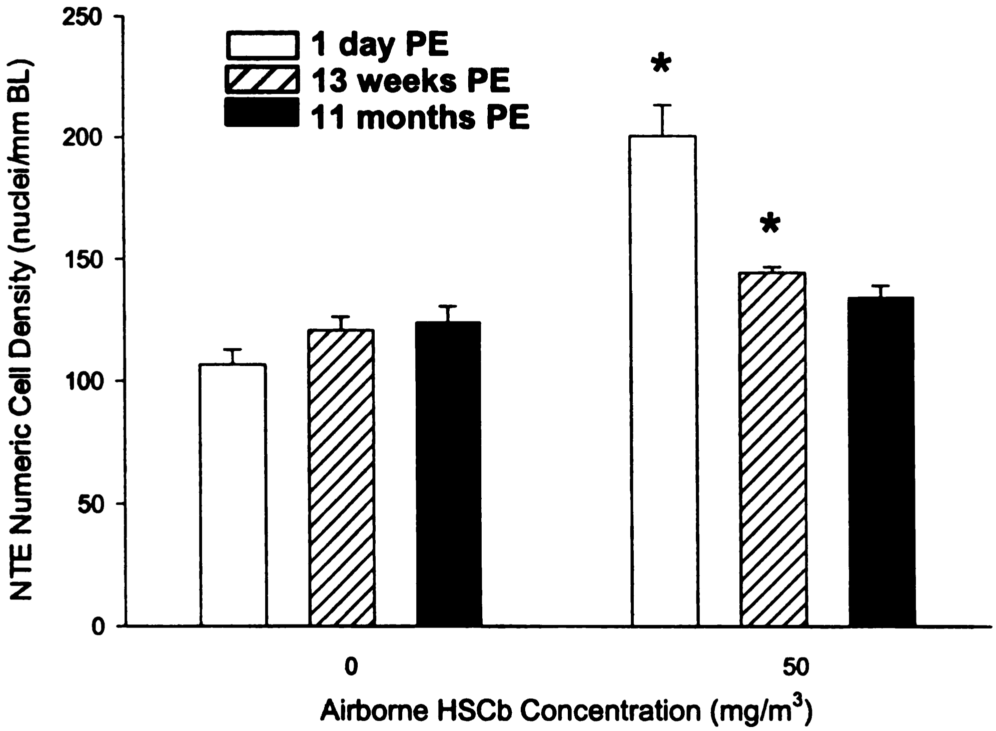

Figure 31: Total Epithelial Cell Density in T1 Maxilloturbinates of Hamsters Exposed to Carbon Black; * = significantly different from respective control group, ($p<0.05$)

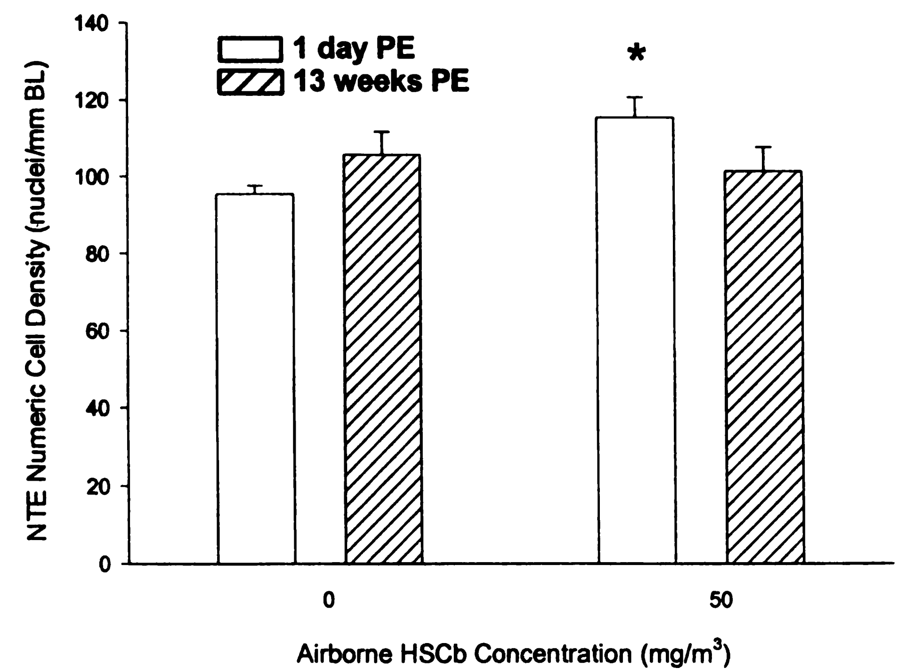

after the end of exposure (Figure 32). Similarly exposed mice had no neutrophils in the midseptum at 13 weeks or 11 months PE.

Hamsters

Hamsters exposed to 50 mg/m^3 HSCb had no neutrophils in the nasal mucosa of the midseptum at any time point after the end of exposure (Figure 32).

Figure 32: Neutrophils in Nasal Mucosa Lining the Midseptum (T2) of Rodents Exposed to Carbon Black at 1 day PE; * = significantly different from respective control group, ($p<0.05$); N/D = not detected

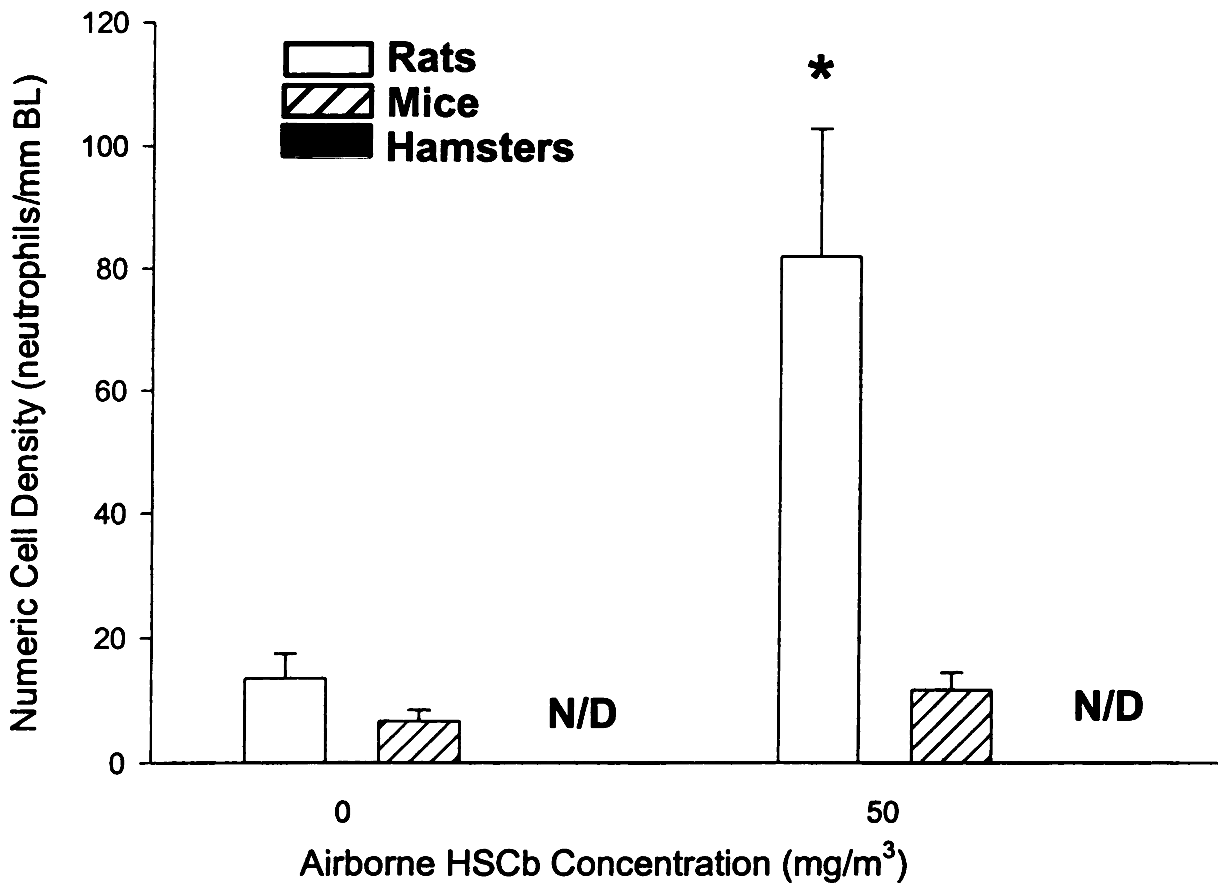

IV. Discussion

The purpose of the present study was to determine whether there are differences among three rodents species in the responses of nasal tissues to the inhalation of carbon black particles. Results indicate that the severity of HSCb-induced nasal lesions is dependent on the species of laboratory rodent, as well as on concentration of HSCb and time after exposure. My previous study showed that rat nasal responses to carbon black inhalation were site-specific, and dependent on the dose and time post-exposure (Chapter 2). The present study shows that a similar nasal dose-response relationship and time PE effect exist in mice and hamsters exposed to HSCb. The majority of HSCb-induced nasal lesions, including MCM and epithelial hyperplasia, were transient in exposed mice and hamsters. Only a mild hyperplastic response was seen at 13 weeks PE in mice exposed to 50 mg/m^3 HSCb, and all hamster lesions had resolved by 13 weeks PE. Also MCM, where present, was dose-dependent in exposed mice and hamsters. The most notable result, however, is that rats had much more severe and persistent nasal lesions than either mice or hamsters in response to HSCb exposure.

Patterns of carbon black-induced nasal lesions described in the present study were similar to those of pulmonary lesions found in these same rodents. Preliminary data indicated greater pulmonary toxicity of HSCb in rats as compared to similarly exposed mice and hamsters [21, 30]. Lung inflammation, as indicated by neutrophil influx, was severe and persistent in rats exposed to high concentrations of HSCb, while mice and hamsters showed minimal or no inflammatory response at any dose of HSCb. Also, type II cell hyperplasia was present through 11 months PE in rats exposed to HSCb, while it was transient in mice and hamsters. Therefore, the patterns of greater severity and persistence of HSCb-induced nasal lesions mimic the toxic effects seen in the lungs of the same rodents.

Many other studies have also shown species differences in pulmonary responses to inhaled particles. The most commonly noted difference in responses is between rats and mice. For example, chronic exposure to DEP and carbon black has been shown to lead to a higher incidence of lung tumors in rats than in mice or hamsters [15, 16, 137]. Other studies have reported that chronic exposure to DEP and TiO_2 lead to more severe and persistent non-neoplastic lesions in rats than in mice or hamsters [15, 75, 137]. Henderson, et al. has reported that lavage and lung antioxidants (e.g., GSH reductase) are found in higher levels in mice than in rats exposed to DEP [138]. It is possible that mice are better able to induce antioxidant protection than rats and are therefore less susceptible to oxidative injury from particles [137]. Another reason may be that macrophages in the lungs of mice are less inflammogenic than those in rats. This hypothesis is supported by Henderson's profile of arachadonic acid metabolites (AAMs), which indicates higher levels of the metabolites in rats than in mice [141]. So an environment with higher levels of AAMs, as is found in rats, may be more likely to stimulate marophages to release inflammatory mediators than an environment with lower levels of AAMs, as is found in mice.

There are many possible reasons why species differences are observed in the present study in terms incidence and severity of nasal lesions. Species differences in regional intranasal deposition of particles and nasal tissue sensitivity may account in part for the difference in severity of nasal responses between rats and mice and hamsters. Site-specific dosimetry of carbon black particles in the nasal airways is necessary to determine whether nasal lesions appear due to dose deposition or the sensitivity of nasal tissue to particle deposition. Anatomical and physiological differences could also contribute to the observed differences. For example, the epithelial surface areas and volumes of the nasal cavities are different among rats, mice, and hamsters. Also, a physiological difference known to be more prominent in mice than in other rodents is the decrease in respiratory rate in response to inhaled nasal toxicants [142]. So perhaps less frequent inhalation of particles can result in a lesser overall exposure and in less severe nasal lesions in murine nasal mucosa compared to that of rats. Finally, the differences could be attributed to differences in host defense systems among the three rodent species. Ultrafine particles are thought to directly induce the formation of reactive oxygen species in pulmonary tissues [59, 78]. Presumably carbon black-induced nasal lesions occur via a similar mechanism. Therefore, rats could be more susceptible to formation of the ROS in nasal tissues than mice or hamsters, or could have a less potent antioxidant defense system than other rodent species.

The severity and persistence of carbon black-induced MCM in the Fischer F344 rats suggest that inhalation of carbon black particles may have the potential to induce similar long-lasting alterations in the nasal airways of humans. However, more dosimetric and mechanistic studies must be conducted to determine which rodent species used in the present study is the best model for assessing human risk for Cb inhalation.

CHAPTER 4

Summary and Conclusions

Summary and Conclusions

Carbon black inhalation exposure commonly occurs both occupationally and environmentally. Companies that produce rubber and automotive products, such as tires and gaskets, utilize carbon black particles in the manufacturing of their products, and workers in these plants are frequently exposed to significant levels of carbon black. Also, carbon black (elemental carbon) is the core component of diesel exhaust particles, which are produced in considerable concentrations in high-traffic regions. Therefore, laboratory animal exposure to carbon black has been examined extensively to assess the compound's pulmonary toxicity. However, prior to the present studies, there has been no report of adverse effects induced by carbon black particles to nasal tissues. The results of this project indicate that long-term exposure to carbon black particles causes chronic pathology in the nasal mucosa of laboratory rodents. Furthermore, the severity and persistence of the nasal pathology was found to be dependent on dose, time post-exposure, particle surface area, and rodent species.

Experimental findings described in Chapter 2 indicate that rat nasal passages are susceptible to toxicity induced by carbon black inhalation. High-surface area carbon black-induced alterations to rat nasal epithelium and underlying lamina propria included MCM, ECH, and a chronic active rhinitis. While the inflammatory response was transient, seen only immediately after the end of exposure, the metaplastic and hyperplastic lesions persisted up to 11 months post-exposure. Additionally, it was found that low-surface area carbon black particles do not induce any nasal lesions in rats.

Results described in Chapter 2 may be used to implicate the low-surface area carbon black particles (Sterling V) used in manufacturing as less toxic to the nasal passages than the high-surface area carbon black particles (Printex 90). Additionally, the severity and persistence of high-surface area carbon black-induced nasal lesions in rats suggest that inhalation of carbon black particles may have the potential to induce similar long-lasting alterations in the nasal airways of humans. However, further study of carbon black toxic potential to the human nose and species comparisons is required to determine how applicable the rat model used in the present study is to human risk assessment.

Species differences in carbon black-induced nasal lesions were described in Chapter 3. Rats had much more severe and persistent MCM and epithelial hyperplasia than either mice or hamsters. Mice had moderate MCM and hyperplasia versus rats similarly exposed to the high concentration of carbon black, while hamsters had only very mild nasal lesions. Neither mice nor hamsters exhibited the acute inflammatory response seen in similarly exposed rats. Also, rat lesions persisted up to 11 months after the end of exposure, while mouse and hamster lesions were only observed immediately post-exposure.

The species difference described in the Chapter 3 study indicates a need to assess the anatomical and physiological differences among the rodent species. Tissue sensitivity and regional particle deposition could also be contributing to the observed species difference. Further dosimetric studies are needed to determine what factors are contributing carbon black nasal toxic sensitivity. Additionally, comparison of these rodent models to monkey and human nasal toxicant models is necessary since the purpose of the research is to assess human risk to carbon black exposure.

Future Directions and Applications

Results of this thesis project provide an initial examination of carbon black as a nasal toxicant, but much more in-depth study of the mechanism of its toxicity is required to understand the implications of the compound in everyday exposure as well as assess the human excess risk factor.

One step to take directly from the results of this study is to determine site-specific dosimetry of the carbon black particles in rodent nasal airways. As previously mentioned, two likely reasons for differences in nasal lesions among the rodent species are regional deposition and tissue sensitivity. Site-specific dosimetry, or measurement of the dose reaching a particular site in the nasal tissue, will allow us to know whether the influence of dose deposition or sensitivity is more prominent. Many other inhaled nasal toxicants are known to exhibit lesions in the nose following patterns that are both site and species specific [143-145]. Dosimetry studies are typically done using computational fluid dynamics (CFD) models of the nasal passages of a certain animal species. Currently models of the rat, monkey, and human noses are being developed in order to determine factors affecting nasal uptake, to make interspecies dosimetric comparisons, and to provide anatomical information [146]. The rat model of course would be most directly applicable to the present study for dose-deposition examination, but the monkey and human models can also be utilized to predict distribution of carbon black-induced nasal lesions in those species.

Since the purpose of the present study is to provide animal models to predict human exposure to carbon black, controlled monkey and human exposures would be a logical next step in the research. Specifically, non-human primate chronic inhalation exposures to carbon black at concentrations similar to those used in the present study would provide knowledge about the differences in susceptibility between rodents and primates. This information could then be used to determine which rodent species used in the present study would be best for estimating the human risk to carbon black-induced nasal toxicity. Additionally, since controlled human exposures to hazardous levels of carbon black may not be possible, in vitro studies of human nasal epithelial cells would be a relevant method of studying toxicity to humans. Examples of in vitro measurements worth examining include the levels of inflammatory cytokines, reactive oxygen species, and antioxidants.

Finally, much work remains to be done in the understanding of mechanisms of carbon black toxicity on the cellular level. Many studies examining the mechanism of ultrafine particle toxicity in the pulmonary airways have determined that the particles can directly induce the formation of reactive oxygen species (ROS). Studies need to be implemented to determine whether particles act via a similar mechanism in nasal tissues. Immunohistochemical staining of nasal tissues from the present study for certain oxidants known to induce oxidative stress would allow us to determine whether there is a correlation between oxidant status and distribution of carbon black-induced nasal lesions in certain regions of nasal tissue.

Overall the results of this thesis project provide insight into the nasal toxic potential of carbon black. The no observable adverse effect level (NOAEL) for HSCb-induced nasal toxicity in this study was 1 mg/m^3. This finding may be used in establishing exposure limits in occupational settings of carbon black manufacturing and use. Additionally, the results can be incorporated into research involving diesel emissions testing of elemental carbon concentrations in high-traffic environments. The present study is the first to report on nasal lesions induced by inhaled carbon black particles, and provides a solid foundation for the study of carbon black nasal toxicity.

BIBLIOGRAPHY

1. Columbian Chemicals Company, T., *Carbon Black Materials Safety Data Sheet.* CCC, Marietta, GA, 2000.

2. Kinney, P.L., et al., *Airborne concentrations of PM(2.5) and diesel exhaust particles on Harlem sidewalks: a community-based pilot study.* Environ Health Perspect, 2000. **108**(3): p. 213-8.

3. Lena, T.S., et al., *Elemental carbon and PM(2.5)levels in an urban community heavily impacted by truck traffic.* Environ Health Perspect, 2002. **110**(10): p. 1009-15.

4. Zaebst, D.D., et al., *Quantitative determination of trucking industry workers' exposures to diesel exhaust particles.* Am Ind Hyg Assoc J, 1991. **52**(12): p. 529-41.

5. USEPA, *Review of EPA's health assessment document for diesel exhaust.* Clean Air Scientific Advisory Committee, EPA-SAB-CASAC-01-003, US Environmental Protection Agency,, 2000.

6. Oberdorster, G., *Significance of particle parameters in the evaluation of exposure-dose-response relationships of inhaled particles.* Inhal Toxicol, 1996. **8 Suppl**: p. 73-89.

7. IARC, *Carbon black.* IARC monographs on the evaluation of carcinogenic risk to humans, 1996. **65**.

8. Muranko, H.J., T.A. Hethmon, and R.G. Smith, *"Total" and respirable dust exposures in the U.S. carbon black manufacturing industry.* Aihaj, 2001. **62**(1): p. 57-64.

9. Teta, M.J., M.G. Ott, and A.R. Schnatter, *Population based mortality surveillance in carbon products manufacturing plants.* Br J Ind Med, 1987. **44**(5): p. 344-50.

10. Parent, M.E., J. Siemiatycki, and G. Renaud, *Case-control study of exposure to carbon black in the occupational setting and risk of lung cancer.* Am J Ind Med, 1996. **30**(3): p. 285-92.

11. Harber, P., et al., *Effect of carbon black exposure on respiratory function and symptoms.* J Occup Environ Med, 2003. **45**(2): p. 144-55.

12. Smith, K.R., et al., *Airborne particles of the california central valley alter the lungs of healthy adult rats.* Environ Health Perspect, 2003. **111**(7): p. 902-8; discussion A408-9.

13. Mauderly, J.L., *Changes in the Composition of Diesel Exhaust Results in Changes in the Magnitude of Several Acute Inhalation Responses.* 2004 Itinerary Planner. Baltimore, MD: Society of Toxicology, 2004.

14. Driscoll, K.E., et al., *Pulmonary inflammatory, chemokine, and mutagenic responses in rats after subchronic inhalation of carbon black.* Toxicol Appl Pharmacol, 1996. **136**(2): p. 372-80.

15. Nikula, K.J., et al., *Comparative pulmonary toxicities and carcinogenicities of chronically inhaled diesel exhaust and carbon black in F344 rats.* Fundam Appl Toxicol, 1995. **25**(1): p. 80-94.

16. Mauderly, J.L., et al., *Pulmonary toxicity of inhaled diesel exhaust and carbon black in chronically exposed rats. Part I: Neoplastic and nonneoplastic lung lesions.* Res Rep Health Eff Inst, 1994(68 Pt 1): p. 1-75; discussion 77-97.

17. Heinrich, U., *Chronic inhalation exposure of Wistar rats and two different strains of mice to diesel engine exhaust, carbon black, and titanium dioxide.* Inhal Toxicol, 1995. **7**: p. 533-556.

18. Rittinghausen, S., U. Mohr, and D.L. Dungworth, *Pulmonary cystic keratinizing squamous cell lesions of rats after inhalation/instillation of different particles.* Exp Toxicol Pathol, 1997. **49**(6): p. 433-46.

19. Ma, J.Y. and J.K. Ma, *The dual effect of the particulate and organic components of diesel exhaust particles on the alteration of pulmonary immune/inflammatory responses and metabolic enzymes.* J Environ Sci Health Part C Environ Carcinog Ecotoxicol Rev, 2002. **20**(2): p. 117-47.

20. Gallagher, J., et al., *Formation of 8-oxo-7,8-dihydro-2'-deoxyguanosine in rat lung DNA following subchronic inhalation of carbon black.* Toxicol Appl Pharmacol, 2003. **190**(3): p. 224-31.

21. Harkema, J.R., *Differential persistence of alveolitis and epithelial proliferation in the lungs of rats and mice exposed to carbon black.* The Toxicologist, 2002. **66**(1-S).

22. Lundborg, M., et al., *Human alveolar macrophage phagocytic function is impaired by aggregates of ultrafine carbon particles.* Environ Res, 2001. **86**(3): p. 244-53.

23. Renwick, L.C., K. Donaldson, and A. Clouter, *Impairment of alveolar macrophage phagocytosis by ultrafine particles.* Toxicol Appl Pharmacol, 2001. **172**(2): p. 119-27.

24. Moller, W., et al., *Ultrafine particles cause cytoskeletal dysfunctions in macrophages.* Toxicol Appl Pharmacol, 2002. **182**(3): p. 197-207.

25. Oberdorster, G., *Lung particle overload: implications for occupational exposures to particles.* Regul Toxicol Pharmacol, 1995. **21**(1): p. 123-35.

26. Gilmour, P.S., et al., *Pulmonary and systemic effects of short-term inhalation exposure to ultrafine carbon black particles.* Toxicol Appl Pharmacol, 2004. **195**(1): p. 35-44.

27. Rengasamy, A., et al., *Diesel exhaust particle-induced alterations of pulmonary phase I and phase II enzymes of rats.* J Toxicol Environ Health A, 2003. **66**(2): p. 153-67.

28. Li, X.Y., et al., *Short-term inflammatory responses following intratracheal instillation of fine and ultrafine carbon black in rats.* Inhal Toxicol, 1999. **11**(8): p. 709-31.

29. Timblin, C.R., et al., *Ultrafine airborne particles cause increases in protooncogene expression and proliferation in alveolar epithelial cells.* Toxicol Appl Pharmacol, 2002. **179**(2): p. 98-104.

30. Elder, A., *Comparative dose-related effects in the lungs of rats and mice following carbon black inhalation.* The Toxicologist, 2002. **66**(1-S).

31. Nau, C.A., G.T. Taylor, and C.H. Lawrence, *Properties and physiological effects of thermal carbon black.* J Occup Med, 1976. **18**(11): p. 732-4.

32. Morrow, P.E., *Possible mechanisms to explain dust overloading of the lungs.* Fundam Appl Toxicol, 1988. **10**(3): p. 369-84.

33. van Beurden, W.J., et al., *Superoxide production by peripheral polymorphonuclear leukocytes in patients with COPD.* Respir Med, 2003. **97**(4): p. 401-6.

34. Kim, H., et al., *Ultrafine carbon black particles inhibit human lung fibroblast-mediated collagen gel contraction.* Am J Respir Cell Mol Biol, 2003. **28**(1): p. 111-21.

35. Don Porto Carero, A., et al., *Genotoxic effects of carbon black particles, diesel exhaust particles, and urban air particulates and their extracts on a human alveolar epithelial cell line (A549) and a human monocytic cell line (THP-1).* Environ Mol Mutagen, 2001. **37**(2): p. 155-63.

36. Al-Humadi, N.H., et al., *The effect of diesel exhaust particles (DEP) and carbon black (CB) on thiol changes in pulmonary ovalbumin allergic sensitized Brown Norway rats.* Exp Lung Res, 2002. **28**(5): p. 333-49.

37. Nilsen, A., R. Hagemann, and I. Eide, *The adjuvant activity of diesel exhaust particles and carbon black on systemic IgE production to ovalbumin in mice after intranasal instillation.* Toxicology, 1997. **124**(3): p. 225-32.

38. van Zijverden, M., et al., *Coadministration of antigen and particles optimally stimulates the immune response in an intranasal administration model in mice.* Toxicol Appl Pharmacol, 2001. **177**(3): p. 174-8.

39. van Zijverden, M., et al., *Diesel exhaust, carbon black, and silica particles display distinct Th1/Th2 modulating activity.* Toxicol Appl Pharmacol, 2000. **168**(2): p. 131-9.

40. Lambert, A.L., et al., *Ultrafine carbon black particles enhance respiratory syncytial virus-induced airway reactivity, pulmonary inflammation, and chemokine expression.* Toxicol Sci, 2003. **72**(2): p. 339-46.

41. Lambert, A.L., et al., *Effect of preexposure to ultrafine carbon black on respiratory syncytial virus infection in mice.* Toxicol Sci, 2003. **72**(2): p. 331-8.

42. Jakab, G.J. and D.R. Hemenway, *Concomitant exposure to carbon black particulates enhances ozone-induced lung inflammation and suppression of alveolar macrophage phagocytosis.* J Toxicol Environ Health, 1994. **41**(2): p. 221-31.

43. Kleinman, M.T., et al., *Toxicity of chemical components of ambient fine particulate matter (PM 2.5) inhaled by aged rats.* J Appl Toxicol, 2000. **20**(5): p. 357-64.

44. Finch, G.L., et al., *Clearance, translocation, and excretion of beryllium following acute inhalation of beryllium oxide by beagle dogs.* Fundam Appl Toxicol, 1990. **15**(2): p. 231-41.

45. Lataillade, G., et al., *Translocation of plutonium from rat and monkey lung after inhalation of industrial plutonium oxide and mixed uranium and plutonium oxide.* Int J Radiat Biol, 1995. **67**(3): p. 373-80.

46. Kreyling, W.G., et al., *Translocation of ultrafine insoluble iridium particles from lung epithelium to extrapulmonary organs is size dependent but very low.* J Toxicol Environ Health A, 2002. **65**(20): p. 1513-30.

47. Sunderman, F.W., Jr., *Nasal toxicity, carcinogenicity, and olfactory uptake of metals.* Ann Clin Lab Sci, 2001. **31**(1): p. 3-24.

48. Oberdorster, G., et al., *Extrapulmonary translocation of ultrafine carbon particles following whole-body inhalation exposure of rats.* J Toxicol Environ Health A, 2002. **65**(20): p. 1531-43.

49. Khandoga, A., et al., *Ultrafine particles exert prothrombotic but not inflammatory effects on the hepatic microcirculation in healthy mice in vivo.* Circulation, 2004. **109**(10): p. 1320-5.

50. Oberdorster, G., *Translocation of ultrafine particles to the brain.* 2004.

51. Gordon, T., et al., *Effects of concentrated ambient particles in rats and hamsters: an exploratory study.* Res Rep Health Eff Inst, 2000(93): p. 5-34; discussion 35-42.

52. Peters, A., et al., *Air pollution and incidence of cardiac arrhythmia.* Epidemiology, 2000. **11**(1): p. 11-7.

53. Seaton, A., et al., *Particulate air pollution and acute health effects.* Lancet, 1995. **345**(8943): p. 176-8.

54. Vincent, R., et al., *Inhalation toxicology of urban ambient particulate matter: acute cardiovascular effects in rats.* Res Rep Health Eff Inst, 2001(104): p. 5-54; discussion 55-62.

55. Sorensen, M., et al., *Personal PM2.5 exposure and markers of oxidative stress in blood.* Environ Health Perspect, 2003. **111**(2): p. 161-6.

56. Mar, T.F., et al., *Associations between air pollution and mortality in Phoenix, 1995-1997.* Environ Health Perspect, 2000. **108**(4): p. 347-53.

57. Metzger, K.B., et al., *Ambient air pollution and cardiovascular emergency department visits.* Epidemiology, 2004. **15**(1): p. 46-56.

58. USEPA, *PM - How Particulate Matter Affects the Way We Live & Breathe.* Office of Air Quality Planning & Standards, US Environmental Protection Agency, 2000.

59. Dick, C.A., et al., *Murine pulmonary inflammatory responses following instillation of size-fractionated ambient particulate matter.* J Toxicol Environ Health A, 2003. **66**(23): p. 2193-2207.

60. Monn, C. and S. Becker, *Cytotoxicity and induction of proinflammatory cytokines from human monocytes exposed to fine (PM2.5) and coarse*

particles (PM10-2.5) in outdoor and indoor air. Toxicol Appl Pharmacol, 1999. **155**(3): p. 245-52.

61. Tao, F., B. Gonzalez-Flecha, and L. Kobzik, *Reactive oxygen species in pulmonary inflammation by ambient particulates.* Free Radic Biol Med, 2003. **35**(4): p. 327-40.

62. Donaldson, K., et al., *Ambient particle inhalation and the cardiovascular system: potential mechanisms.* Environ Health Perspect, 2001. **109 Suppl 4**: p. 523-7.

63. Schins, R.P., et al., *Inflammatory effects of coarse and fine particulate matter in relation to chemical and biological constituents.* Toxicol Appl Pharmacol, 2004. **195**(1): p. 1-11.

64. Hetland, R.B., et al., *Release of inflammatory cytokines, cell toxicity and apoptosis in epithelial lung cells after exposure to ambient air particles of different size fractions.* Toxicol In Vitro, 2004. **18**(2): p. 203-12.

65. Donaldson, K., et al., *Oxidative stress and calcium signaling in the adverse effects of environmental particles (PM10).* Free Radic Biol Med, 2003. **34**(11): p. 1369-82.

66. Pope, C.A., 3rd, D.V. Bates, and M.E. Raizenne, *Health effects of particulate air pollution: time for reassessment?* Environ Health Perspect, 1995. **103**(5): p. 472-80.

67. Osornio-Vargas, A.R., et al., *Proinflammatory and cytotoxic effects of Mexico City air pollution particulate matter in vitro are dependent on particle size and composition.* Environ Health Perspect, 2003. **111**(10): p. 1289-93.

68. Choi, J.H., et al., *Comparative study of PM2.5 - and PM10 - induced oxidative stress in rat lung epithelial cells.* J Vet Sci, 2004. **5**(1): p. 11-8.

69. Calderon-Garciduenas, L., et al., *Canines as sentinel species for assessing chronic exposures to air pollutants: part 2. Cardiac pathology.* Toxicol Sci, 2001. **61**(2): p. 356-67.

70. *Ultrafine particles: insidious invaders.* Arch Dis Child, 2002. **86**(4): p. 290.

71. Huang, S.L., M.K. Hsu, and C.C. Chan, *Effects of submicrometer particle compositions on cytokine production and lipid peroxidation of human bronchial epithelial cells.* Environ Health Perspect, 2003. **111**(4): p. 478-82.

72. Oberdorster, G., *Pulmonary effects of inhaled ultrafine particles.* Int Arch Occup Environ Health, 2001. **74**(1): p. 1-8.

73. Nikula, K.J., *Rat lung tumors induced by exposure to selected poorly soluble nonfibrous particles.* Inhal Toxicol, 2000. **12**(1-2): p. 97-119.

74. Lee, K.P., H.J. Trochimowicz, and C.F. Reinhardt, *Pulmonary response of rats exposed to titanium dioxide (TiO2) by inhalation for two years.* Toxicol Appl Pharmacol, 1985. **79**(2): p. 179-92.

75. Bermudez, E., et al., *Long-term pulmonary responses of three laboratory rodent species to subchronic inhalation of pigmentary titanium dioxide particles.* Toxicol Sci, 2002. **70**(1): p. 86-97.

76. Oberdorster, G., *Toxicokinetics and effects of fibrous and nonfibrous particles.* Inhal Toxicol, 2002. **14**(1): p. 29-56.

77. Oberdorster, G., J. Ferin, and B.E. Lehnert, *Correlation between particle size, in vivo particle persistence, and lung injury.* Environ Health Perspect, 1994. **102 Suppl 5**: p. 173-9.

78. Brown, D.M., et al., *Size-dependent proinflammatory effects of ultrafine polystyrene particles: a role for surface area and oxidative stress in the enhanced activity of ultrafines.* Toxicol Appl Pharmacol, 2001. **175**(3): p. 191-9.

79. Hohr, D., et al., *The surface area rather than the surface coating determines the acute inflammatory response after instillation of fine and ultrafine TiO2 in the rat.* Int J Hyg Environ Health, 2002. **205**(3): p. 239-44.

80. Donaldson, K., et al., *The pulmonary toxicology of ultrafine particles.* J Aerosol Med, 2002. **15**(2): p. 213-20.

81. MacNee, W. and K. Donaldson, *Mechanism of lung injury caused by PM10 and ultrafine particles with special reference to COPD.* Eur Respir J Suppl, 2003. **40**: p. 47s-51s.

82. Li, N., et al., *Ultrafine particulate pollutants induce oxidative stress and mitochondrial damage.* Environ Health Perspect, 2003. **111**(4): p. 455-60.

83. Brown, D.M., et al., *Calcium and ROS-mediated activation of transcription factors and TNF-alpha cytokine gene expression in macrophages exposed to ultrafine particles.* Am J Physiol Lung Cell Mol Physiol, 2004. **286**(2): p. L344-53.

84. Fischer, B.M. and J.A. Voynow, *Neutrophil elastase induces MUC5AC gene expression in airway epithelium via a pathway involving reactive oxygen species.* Am J Respir Cell Mol Biol, 2002. **26**(4): p. 447-52.

85. Rose, M.C., T.J. Nickola, and J.A. Voynow, *Airway mucus obstruction: mucin glycoproteins, MUC gene regulation and goblet cell hyperplasia.* Am J Respir Cell Mol Biol, 2001. **25**(5): p. 533-7.

86. Wagner, J.G., J.A. Hotchkiss, and J.R. Harkema, *Enhancement of nasal inflammatory and epithelial responses after ozone and allergen coexposure in Brown Norway rats.* Toxicol Sci, 2002. **67**(2): p. 284-94.

87. Whittaker, L., et al., *Interleukin-13 mediates a fundamental pathway for airway epithelial mucus induced by CD4 T cells and interleukin-9.* Am J Respir Cell Mol Biol, 2002. **27**(5): p. 593-602.

88. Nadel, J.A., *Role of epidermal growth factor receptor activation in regulating mucin synthesis.* Respir Res, 2001. **2**(2): p. 85-9.

89. Morgan, K.T. and T.M. Monticello, *Airflow, gas deposition, and lesion distribution in the nasal passages.* Environ Health Perspect, 1990. **85**: p. 209-18.

90. Hubbs, A.F., et al., *Necrosis of nasal and airway epithelium in rats inhaling vapors of artificial butter flavoring.* Toxicol Appl Pharmacol, 2002. **185**(2): p. 128-35.

91. Harkema, J.R. and J.G. Wagner, *Non-allergic models of mucous cell metaplasia and mucus hypersecretion in rat nasal and pulmonary airways.* Novartis Found Symp, 2002. **248**: p. 181-97; discussion 197-200, 277-82.

92. Harkema, J.R., et al., *Long-lasting effects of chronic ozone exposure on rat nasal epithelium.* Am J Respir Cell Mol Biol, 1999. **20**(3): p. 517-29.

93. Morgan, K.T., *A brief review of formaldehyde carcinogenesis in relation to rat nasal pathology and human health risk assessment.* Toxicol Pathol, 1997. **25**(3): p. 291-307.

94. Min, Y.G., et al., *Histopathologic changes in the olfactory epithelium in mice after exposure to sulfur dioxide.* Acta Otolaryngol, 1994. **114**(4): p. 447-52.

95. Harkema, J.R., J.A. Hotchkiss, and R.F. Henderson, *Effects of 0.12 and 0.80 ppm ozone on rat nasal and nasopharyngeal epithelial mucosubstances: quantitative histochemistry.* Toxicol Pathol, 1989. **17**(3): p. 525-35.

96. Harkema, J.R. and J.L. Mauderly, *Consequences of prolonged inhalation of ozone on F344/N rats: collaborative studies. Part V: Effects on pulmonary function.* Res Rep Health Eff Inst, 1994(65 Pt 5): p. 3-17; discussion 19-26.

97. Harkema, J.R., P.J. Catalano, and J.A. Hotchkiss, *Consequences of prolonged inhalation of ozone on F344/N rats: collaborative studies. Part XII: Atrophy of bone in nasal turbinates.* Res Rep Health Eff Inst, 1997(65 (Pt 12)): p. 1-19; discussion 21-6.

98. Johnson, N.F., et al., *Proliferative responses of rat nasal epithelia to ozone.* Toxicol Appl Pharmacol, 1990. **103**(1): p. 143-55.

99. Hotchkiss, J.A., J.R. Harkema, and N.F. Johnson, *Kinetics of nasal epithelial cell loss and proliferation in F344 rats following a single exposure to 0.5 ppm ozone.* Toxicol Appl Pharmacol, 1997. **143**(1): p. 75-82.

100. Harkema, J.R., et al., *Response of the macaque nasal epithelium to ambient levels of ozone. A morphologic and morphometric study of the transitional and respiratory epithelium.* Am J Pathol, 1987. **128**(1): p. 29-44.

101. Harkema, J.R., et al., *Effects of an ambient level of ozone on primate nasal epithelial mucosubstances. Quantitative histochemistry.* Am J Pathol, 1987. **127**(1): p. 90-6.

102. Folinsbee, L.J., et al., *Respiratory responses to repeated prolonged exposure to 0.12 ppm ozone.* Am J Respir Crit Care Med, 1994. **149**(1): p. 98-105.

103. Graham, D., F. Henderson, and D. House, *Neutrophil influx measured in nasal lavages of humans exposed to ozone.* Arch Environ Health, 1988. **43**(3): p. 228-33.

104. Carson, J.L., et al., *Response of human ciliated respiratory epithelium to brief in vivo ozone exposure: an ultrastructural study.* Environ Res, 1985. **37**(1): p. 212-27.

105. Georgieva, A.V., J.S. Kimbell, and P.M. Schlosser, *A distributed-parameter model for formaldehyde uptake and disposition in the rat nasal lining.* Inhal Toxicol, 2003. **15**(14): p. 1435-63.

106. Woutersen, R.A., et al., *Nasal tumours in rats after severe injury to the nasal mucosa and prolonged exposure to 10 ppm formaldehyde.* J Appl Toxicol, 1989. **9**(1): p. 39-46.

107. Swenberg, J.A., et al., *Induction of squamous cell carcinomas of the rat nasal cavity by inhalation exposure to formaldehyde vapor.* Cancer Res, 1980. **40**(9): p. 3398-402.

108. Casanova, M., et al., *Covalent binding of inhaled formaldehyde to DNA in the respiratory tract of rhesus monkeys: pharmacokinetics, rat-to-monkey interspecies scaling, and extrapolation to man.* Fundam Appl Toxicol, 1991. **17**(2): p. 409-28.

109. Monticello, T.M. and K.T. Morgan, *Cell proliferation and formaldehyde-induced respiratory carcinogenesis.* Risk Anal, 1994. **14**(3): p. 313-9.

110. Recio, L., et al., *p53 mutations in formaldehyde-induced nasal squamous cell carcinomas in rats.* Cancer Res, 1992. **52**(21): p. 6113-6.

111. Morris, J.B., *Dosimetry, toxicity and carcinogenicity of inspired acetaldehyde in the rat.* Mutat Res, 1997. **380**(1-2): p. 113-24.

112. Brenneman, K.A., et al., *Olfactory mucosal necrosis in male CD rats following acute inhalation exposure to hydrogen sulfide: reversibility and the possible role of regional metabolism.* Toxicol Pathol, 2002. **30**(2): p. 200-8.

113. Wolf, D.C., et al., *Two-year inhalation exposure of female and male B6C3F1 mice and F344 rats to chlorine gas induces lesions confined to the nose.* Fundam Appl Toxicol, 1995. **24**(1): p. 111-31.

114. Boland, S., et al., *Diesel exhaust particles are taken up by human airway epithelial cells in vitro and alter cytokine production.* Am J Physiol, 1999. **276**(4 Pt 1): p. L604-13.

115. Kelly, J.T., J.S. Kimbell, and B. Asgharian, *Deposition of fine and coarse aerosols in a rat nasal mold.* Inhal Toxicol, 2001. **13**(7): p. 577-88.

116. Martonen, T.B., et al., *Fine particle deposition within human nasal airways.* Inhal Toxicol, 2003. **15**(4): p. 283-303.

117. Diaz-Sanchez, D., et al., *Nasal challenge with diesel exhaust particles can induce sensitization to a neoallergen in the human mucosa.* J Allergy Clin Immunol, 1999. **104**(6): p. 1183-8.

118. Diaz-Sanchez, D., M. Penichet-Garcia, and A. Saxon, *Diesel exhaust particles directly induce activated mast cells to degranulate and increase histamine levels and symptom severity.* J Allergy Clin Immunol, 2000. **106**(6): p. 1140-6.

119. IARC, *Wood dust.* IARC monographs on the evaluation of carcinogenic risk to humans, 1995. **62**.

120. Klintenberg, C., et al., *Adenocarcinoma of the ethmoid sinuses. A review of 28 cases with special reference to wood dust exposure.* Cancer, 1984. **54**(3): p. 482-8.

121. Hayes, R.B., et al., *Wood-related occupations, wood dust exposure, and sinonasal cancer.* Am J Epidemiol, 1986. **124**(4): p. 569-77.

122. Jansing, P.J., et al., *Profiles of occupational exposure in patients with wood dust-induced nasal carcinoma.* Int J Occup Med Environ Health, 2003. **16**(4): p. 329-35.

123. Klein, R.G., et al., *Carcinogenicity assays of wood dust and wood additives in rats exposed by long-term inhalation.* Int Arch Occup Environ Health, 2001. **74**(2): p. 109-18.

124. Baulig, A., et al., *Involvement of reactive oxygen species in the metabolic pathways triggered by diesel exhaust particles in human airway epithelial cells.* Am J Physiol Lung Cell Mol Physiol, 2003. **285**(3): p. L671-9.

125. Hiruma, K., et al., *Effect of diesel exhaust on guinea pig nasal mucosa.* Ann Otol Rhinol Laryngol, 1999. **108**(6): p. 582-8.

126. Gluck, U., R. Schutz, and J.O. Gebbers, *Cytopathology of the nasal mucosa in chronic exposure to diesel engine emission: a five-year survey of Swiss customs officers.* Environ Health Perspect, 2003. **111**(7): p. 925-9.

127. *NTP Toxicology and Carcinogenesis Studies of Talc (CAS No. 14807-96-6)(Non-Asbestiform) in F344/N Rats and B6C3F1 Mice (Inhalation Studies).* Natl Toxicol Program Tech Rep Ser, 1993. **421**: p. 1-287.

128. Calderon-Garciduenas, L., et al., *8-hydroxy-2'-deoxyguanosine, a major mutagenic oxidative DNA lesion, and DNA strand breaks in nasal respiratory epithelium of children exposed to urban pollution.* Environ Health Perspect, 1999. **107**(6): p. 469-74.

129. Calderon-Garciduenas, L., et al., *Cell proliferation in nasal respiratory epithelium of people exposed to urban pollution.* Carcinogenesis, 1999. **20**(3): p. 383-9.

130. Calderon-Garciduenas, L., et al., *Ultrastructural nasal pathology in children chronically and sequentially exposed to air pollutants.* Am J Respir Cell Mol Biol, 2001. **24**(2): p. 132-8.

131. Calderon-Garciduenas, L., et al., *Nasal biopsies of children exposed to air pollutants.* Toxicol Pathol, 2001. **29**(5): p. 558-64.

132. Oberdorster, G., *Effects of subchronically inhaled carbon black in rats, mice, and hamsters: Part II- Inflammation and oxidative stress.* 2004.

133. Young, J.T., *Histopathologic examination of the rat nasal cavity.* Fundam Appl Toxicol, 1981. **1**(4): p. 309-12.

134. Hewett, J.A., et al., *Neutrophil depletion protects against liver injury from bacterial endotoxin.* Lab Invest, 1992. **66**(3): p. 347-61.

135. Hotchkiss, J.A., J.R. Harkema, and R.F. Henderson, *Effect of cumulative ozone exposure on ozone-induced nasal epithelial hyperplasia and secretory metaplasia in rats.* Exp Lung Res, 1991. **17**(3): p. 589-600.

136. Kiviluoto, M., et al., *Effects of vanadium on the upper respiratory tract of workers in a vanadium factory. A macroscopic and microscopic study.* Scand J Work Environ Health, 1979. **5**(1): p. 50-8.

137. Mauderly, J.L., et al., *Diesel exhaust is not a pulmonary carcinogen in CD-1 mice exposed under conditions carcinogenic to F344 rats.* Fundam Appl Toxicol, 1996. **30**(2): p. 233-42.

138. Henderson, R.F., et al., *Response of rodents to inhaled diluted diesel exhaust: biochemical and cytological changes in bronchoalveolar lavage fluid and in lung tissue.* Fundam Appl Toxicol, 1988. **11**(3): p. 546-67.

139. Nikula, K.J., et al., *Sites of particle retention and lung tissue responses to chronically inhaled diesel exhaust and coal dust in rats and cynomolgus monkeys.* Environ Health Perspect, 1997. **105 Suppl 5**: p. 1231-4.

140. Ward, J.M., et al., *Hyalinosis and Ym1/Ym2 gene expression in the stomach and respiratory tract of 129S4/SvJae and wild-type and CYP1A2-null B6, 129 mice.* Am J Pathol, 2001. **158**(1): p. 323-32.

141. Henderson, R.F., et al., *Species differences in release of arachidonate metabolites in response to inhaled diluted diesel exhaust.* Toxicol Lett, 1988. **42**(3): p. 325-32.

142. Gagnaire, F., et al., *Comparison of the sensory irritation response in mice to chlorine and nitrogen trichloride.* J Appl Toxicol, 1994. **14**(6): p. 405-9.

143. Kimbell, J.S., et al., *Dosimetry modeling of inhaled formaldehyde: comparisons of local flux predictions in the rat, monkey, and human nasal passages.* Toxicol Sci, 2001. **64**(1): p. 100-10.

144. Moulin, F.J., et al., *Predicted regional flux of hydrogen sulfide correlates with distribution of nasal olfactory lesions in rats.* Toxicol Sci, 2002. **66**(1): p. 7-15.

145. Frederick, C.B., et al., *A hybrid computational fluid dynamics and physiologically based pharmacokinetic model for comparison of predicted tissue concentrations of acrylic acid and other vapors in the rat and human nasal cavities following inhalation exposure.* Inhal Toxicol, 2001. **13**(5): p. 359-76.

146. Kimbell, J.S. and R.P. Subramaniam, *Use of computational fluid dynamics models for dosimetry of inhaled gases in the nasal passages.* Inhal Toxicol, 2001. **13**(5): p. 325-34.